ENCLOSURE 2

APP-GW-GLR-044 Rev. 2 (TR85) "Nuclear Island Basemat and Foundation"

APP-GW-GLR-044
Revision 2

February 2011

AP1000 Standard Combined License Technical Report

Nuclear Island Basemat and Foundation

Westinghouse Electric Company LLC
Nuclear Power Plants
Post Office Box 355
Pittsburgh, PA 15230-0355

Record of Revisions

Rev	Date	Revision Description[1]
0	See EDMS	Original Issue
1	Jan. 2009	Road Map created to track changes and additions to Rev 1
2	February 2011	Road Map created to track changes and additions to Rev 2

Note (1) Significant changes are briefly described in this table. In the rest of the calc note, each row that has changed is marked using a revision bar in the margin of the page. This approach satisfies the change identification requirements in WP 4.5 Section 7.4. The Record of Revisions for older revisions should be deleted as necessary to limit this table to one page.

Road Map of Changes from Rev. 0 to Rev. 1 for TR85 (APP-GW-GLR-044)

Item	Rev. 0 Section Number	Change in Rev. 1	Reason for Change
1	1.0 Introduction	Delete "final" in 3rd sentence of 1st paragraph: "This report summarizes the design of the - - "	Addresses comments of RAI-TR85-SEB1-01 to clarify "final design".
2	2.4.1 2D SASSI analysis	Modified all paragraphs to reference updates and changes per RAIs	Addresses comments and includes revisions as presented in RAI-TR85-SEB1-05 R2, -06 and -10.
3	2.4.2 2D ANSYS non-linear dynamic analysis	Modified all paragraphs, except the 1st and 3rd (from Rev. 0) to reference updates and changes per RAIs	Addresses comments and includes revisions as presented in RAI-TR85-SEB1-05 R2, -12 and -14.
4	2.4.3 Site interface for soil	Became Section 2.4.4, see below	Inserted Sec. 2.4.3, 3D SASSI Analysis
5	2.4.3 3D SASSI Analysis (new section)	Description and results from new 3D SASSI analyses	As proposed in RAI-TR85-SEB1-03
6	2.4.4 Site interface for soil	• Modify value for "Average Allowable Static Bearing Capacity" from 8,600 lb/ft^2 in Rev. 0 to 8,900 lb/ft^2 in RAI-SRP2.5-RGS1-09 • Add "or, Site specific analysis demonstrate factor of safety appropriate for normal plus safe shutdown earthquake loads." to definition of "Maximum Allowable Dynamic Bearing Capacity for Normal Plus SSE" as in DCD, Table 2-1 (RAI-32) • Modified 3rd paragraph to include reference to DCD, Rev. 17 (RAI-16).	• RAI-SRP2.5-RGS1-09 reflects enhanced shield building design. • Include revision as presented in RAI-TR85-SEB1-16 and -32. Change section reference from 2.4.3 to 2.4.4 • .
7	Tables 2.4-1 and -2	Revisions to results presented in Tables 2.4-1and -2.	Changes presented in RAI-TR85-SEB1-05 and -07 to reflect 2D analysis with enhanced shield building.
8	Tables 2.4-3, -4 and -5 (new tables)	New tables: • Table 2.4-3, Soil Properties in ANSYS Model • Table 2.4-4, Comparison of member forces in ASB stick at elevation 99' from 2D SASSI and ANSYS analyses • Table 2.4-5, SASSI 3D Maximum Bearing Pressure.	• Tables -3 and -4 presented in RAI-TR85-SEB1-05. • Table -5 as a part of RAI-TR85-SEB1--03.
9	Figures 2.4-1through -6	Seven new or revised Figures 2.4-_: • 1, SASSI Basement Model (YZ plane). • 2, East-West 2D SASSI Model in Y Direction. • 3, Generic Soil Profiles; a) low strain values and b) degraded values for SSE analyses. • 4, ANSYS lift-Off Model.	• Changes presented in RAI-TR85-SEB1-05 to reflect 2D SASSI and ANSYS analyses and representative soil models, Figures -1 thru -6. • Figure -7 as a part of RAI-TR85-SEB1-32.

Item	Rev. 0 Section Number	Change in Rev. 1	Reason for Change
		• 5, Comparison of SASSI and ANSYS FRS for Soft to Medium Soil. • 6, 2D ANSYS Time History of Basement Edges: Hard Rock, UBSM Soil, and SM Soil.	
10	2.5 Analysis of settlement during construction	Seventh paragraph: replace "However, this may require redistribution of:" in last paragraph with "The member forces in these analyses are those due to primary externally applied loads and do not consider secondary stresses and strains - - "	Addresses comments of RAI-TR85-SEB1-19.
11	2.6 Nuclear island basement design	• Edited 4th sentence of 1st paragraph to include" and 2.6-2 (a) thru (d)." • Add 7 new paragraphs	Addresses comments and includes revisions as presented in RAI-TR85-SEB1-21 and -22.
12	2.6.1.1 Subgrade modulus	• Edited text in 2nd (RAI-05, -20 and -22) paragraph. • Revised subgrade modulus values in 5th (RAI-22) paragraph.	Addresses comments and includes revisions as presented in RAI-TR85-SEB1-05, -20 and -22.
13	2.6.1.2 Equivalent static accelerations	• Edited text in 1st paragraph to note hard rock and shield building changes. • Added new 2nd paragraph to note NI20 model. • Revised 3rd paragraph NI20 model and basemat reactions.	Addresses comments and includes revisions as presented in RAI-TR85-SEB1 -22.
14	2.6.1.4 Normal plus seismic reactions	• Added 2 new sentences after the 2nd sentence of Rev 0 to discuss clarify overturning cases.	Comments presented in RAI-TR85-SEB1-27 R4.
15	2.6.2 Basement reinforcement design	• Revisions to equations 1, 3, 9 and 10 presented in the 2nd paragraph.	Comments presented in RAI-TR85-SEB1-28, DCD LC10 and DCD LC 11.
16	Table 2.6-1	• Revised subgrade moduli values for the four Rev 0 soil/rock • Increase table to 9 soil/rock cases.	Changes presented in RAI-TR85-SEB1-05
17	Table 2.6-2	• Created Table 2.6-2 (a), Equivalent Seismic Static Accelerations for Nuclear Island Basemat Analysis. • Modified Table 2.6-2 to 2.6-2 (b) by: o deleting Time History values for "Hard Rock" and "2D Analysis" o replacing with Fixed Base Time History Analysis (NI20, all soils) • Created Table 2.6-2 (c), Maximum soil bearing pressures (ksf) at corners from basemat reactions.	Changes presented in RAI-TR85-SEB1-22
18	Table 2.6-4	• Expanded number of layers detailed in table	Changes presented in RAI-TR85-SEB1-30
19	Figure 2.6-2	• Added parts to 2.6-2 (_): o 2.6-2 (a) Section View of NI05 Model from East o 2.6-2 (b) Section View of NI05 Model from North o 2.6-2 (c) Typical Connection of Auxiliary Building Dish o 2.6-2 (d) Connection Nodes between of Containment vessel and Dish	Changes presented in RAI-TR85-SEB1-22

Item	Rev. 0 Section Number	Change in Rev. 1	Reason for Change
		○ 2.6-2 (e) Basemat response spectra from SASSI analyses ○ 2.6-2 (f) Comparison of Time History Response Spectra against "ASB 60.5" envelope	
20	Figures 2.6-9 and -10	• Modified to reflect changes in Table 2.6-4	Changes presented in RAI-TR85-SEB1-30
21	2.9 Nuclear island stability	• Added new 1st and 2nd paragraphs as per RAI-04 • Various revisions to 4th paragraph as per RAI-10	Addresses revisions and deletions as presented in RAI-TR85-SEB1-04 -10 and -34.
22	Table 2.9-1	• Revised factors of safety for SSE Event and modified notes	Changes presented in RAI-TR85-SEB1-10
23	Table 2.9-2	• New table, Factors to Apply to Hard Rock Analysis Base Reactions	Presented in RAI-TR85-SEB1-04
24	Figures 2.9-1 and -2	• New figures, ○ -1, Passive Pressure versus Deflection at Grade (North-South Excitation) ○ -2, Passive Pressure versus Deflection at Grade (East-West Excitation)	Presented in RAI-TR85-SEB1-10
25	5.0 DCD MARK UP	Deleted DCD 17 revisions, added Post Revision 17 Revisions per RAIs	Per RAI-TR85-SEB1-04, -10, -28, -32, -35, -36 and -37.

Road Map of Changes from Rev. 1 to Rev. 2 for TR85 (APP-GW-GLR-044)

Item	Rev. 1 Section Number	Change in Rev. 2	Reason for Change
1	Figures 2.1-1 to 2.1-3	Figures are removed and a reference given to AP1000 DCD figures	Figures are considered Security-Related Information, Withhold Under 10 CFR 2.390d
2	2.2 and 4.0	Removed reference to AP600 DCD Reference 4	Removed reference to DCD
3	2.3.1, 2.6.2 and 4.0	Removed reference to AP1000 DCD Reference 1	Removed reference to DCD
4	2.4.1	Added "Horizontal" to 3rd paragraph	NRC TR85 action item 1
5	2.4.4	Removed "Maximum Allowable" from "Maximum Allowable Dynamics Bearing Capacity for Normal Plus SSE."	Made consistent with AP1000 DCD requirements as given in Chapter 2, Table 2-1.
6	Table 2.6-2(b), 2.6-2(c), and Table 2.6-4	Revised Table 2.6-2(c), Footnote in Table 2.6 (b) and Table 2.6-4 as shown in RAI	Incorporates comments from RAI-TR85-SEB1-32 R5
7	2.9	Revised text per RAI and to indicate that the friction value is based on the governing angle of internal friction, removed statement related to quality requirements for backfill, editorial change referring to 35 degrees.	Incorporates comments from RAI-TR85-SEB1-10 R6; NRC TR85 action item 2, 3, 4 and 5
8	Table 2.9-1	Revised Table and Footnote per RAI	Incorporates comments from RAI-TR85-SEB1-10 R6; NRC TR85 action item 4
9	5.0	Deleted Section related to DCD markups	This section has been deleted from TR85 due to DCD Rev 18's formal submittal and DCD Rev 19 is to be issued shortly

- Note – NRC action items are documented in WEC_WEC_000069

TABLE OF CONTENTS

1.0 INTRODUCTION

The AP1000 design has been certified for application at a hard rock site. Seismic analyses of the AP1000 at soil sites are described in Reference 3. This report summarizes the design of the nuclear island basemat and exterior walls below grade for both hard rock and soil sites. It describes interface demands to be satisfied at a site.

The AP1000 Design Certification Document (DCD) includes COL information items and ITAAC that require reconciliation of the as-built structure to information and criteria included in the DCD and to analyses supporting the DCD. This report provides an updated baseline for the as-designed configuration and validates the basemat and foundation design against the updated seismic spectra and foundation conditions.

COL Information Item 3.7-4 and ITAAC 2. a) i) in Tier 1 Section 3.3 apply to the design and analysis of the structures addressed in this report.

COL Information Item 3.7-4 (NRC FSER Combined License Action Item 3.7.5-1) is associated with the as-built reconciliation of seismic analyses and is as follows:

> The Combined License applicant will reconcile the seismic analyses described in subsection 3.7.2 for detail design changes at rock sites such as those due to as-procured equipment information. Deviations are acceptable based on an evaluation consistent with the methods and procedure of Section 3.7 provided the amplitude of the seismic floor response spectra including the effect due to these deviations, do not exceed the design basis floor response spectra by more than 10 percent

The COL item as written requires as-built information and cannot be satisfied at the Time of COL Application. This timing issue is addressed in a separate technical report. The information in this report validates that the design of the subject structures is acceptable for the updated seismic spectra and foundation conditions at COL application.

ITAAC 2.a) i) in Tier 1 Section 3.3 provides for verification of critical sections of the nuclear island structure. This ITAAC is included in DCD Tier 1, Table 3.3-6 and provided below. These critical sections include the basemat covered by this report. The information in this report validates that the design of the subject structures can satisfy the acceptance criteria. This technical report does not require that the ITAAC be revised.

Design Commitment	Inspections, Tests, Analyses	Acceptance Criteria
2.a) The nuclear island structures, including the critical sections listed in Table 3.3-7, are seismic Category I and are designed and constructed to withstand design basis loads as specified in the Design Description, without loss of structural integrity and the safety-related functions.	i) An inspection of the nuclear island structures will be performed. Deviations from the design due to as-built conditions will be analyzed for the design basis loads.	i) A report exists which reconciles deviations during construction and concludes that the as-built nuclear island structures, including the critical sections, conform to the approved design and will withstand the design basis loads specified in the Design Description without loss of structural integrity or the safety-related functions.

2.0 TECHNICAL BACKGROUND

2.1 Description of Nuclear Island Basemat and Embedded Portion

The nuclear island structures, consisting of the containment building, shield building, and auxiliary building, are founded on a common, cast-in-place, reinforced concrete basemat. Figure 2.1-1 shows a plan view of the AP1000 basemat and Figures 2.1-2 and 2.1-3 show cross section views at the containment center line. The basemat below the auxiliary building is 6 feet thick. Below the shield and containment building, the thickness of the basemat varies from 6 feet at the center to 22 feet under the annular tunnel to 39′-6″ on the west side where there is no tunnel. The nuclear island is embedded to a depth of 39′-6″ below nominal plant grade at elevation 100′. The bottom of the foundation is at elevation 60′-6″.

The plan view footprint is the same as the AP600. The section views are also similar to the AP600. The height of the AP1000 shield building and containment vessel is increased by 25′-6″. The shield walls around the reactor coolant loop in the containment internal structures are a few feet higher. The annular tunnel is full circumference in the AP600 and is eliminated on the west side for the AP1000.

The auxiliary building is a concrete shear-wall structure consisting of vertical shear/bearing walls and horizontal floor slabs. It wraps around approximately 50 percent of the circumference of the shield building. Walls are spaced 18 to 25 feet apart. The floor slabs and the structural walls of the auxiliary building are structurally connected to the cylindrical section of the shield building. The walls carry the vertical loads from the structure to the basemat. Lateral loads are transferred to the walls by the roof and floor slabs. The walls then transmit the loads to the basemat. The walls also provide stiffness to the basemat and distribute the foundation loads between them. This configuration of the structures above the basemat, in combination with the basemat, provides an efficient overall structure.

Adjoining buildings, such as the radwaste building, turbine building, and annex building are structurally separated from the nuclear island structures by a 2-inch gap at and below the grade. A 4-inch minimum gap is provided above grade. This provides space to prevent interaction between the nuclear island structures and the adjacent structures during a seismic event.

Resistance to sliding of the concrete basemat foundation is provided by passive soil pressure and soil friction. This provides the required factor of safety against lateral movement under the most stringent loading conditions.

Plant north is defined toward the turbine building so that the wall on line number 11 (see Figure 2.1-1) is the north wall. The plant coordinate system is defined with X north, Y west, and Z vertical.

**Figure is not shown since it is considered
Security-Related Information, Withhold Under 10 CFR 2.390d**

See AP1000 Design Control Document Figures 3.7.2-12 (Sheet 1 of 12)

Figure 2.1-1

**Nuclear Island Key Structural Dimensions
Plan at El. 66′-6″**

**Figure is not shown since it is considered
Security-Related Information, Withhold Under 10 CFR 2.390d**

See AP1000 Design Control Document Figures 3.7.2-12 (Sheet 8 of 12)

Figure 2.1-2

**Nuclear Island Key Structural Dimensions
Section A - A**

Figure is not shown since it is considered Security-Related Information, Withhold Under 10 CFR 2.390d

See AP1000 Design Control Document Figures 3.7.2-12 (Sheet 9 of 12)

Figure 2.1-3

Nuclear Island Key Structural Dimensions
Section B - B

2.2 AP600 certified design for hard rock and soil sites

This section summarizes the design of the AP600 basemat and foundation. The methodology approved for the design of the AP600 forms the basis for the methodology applied in the design of the AP1000 basemat for soil sites. This design is applicable for sites with the nuclear island founded on soil having a shear wave velocity greater than 1000 feet per second.

2.2.1 AP600 basemat analyses and design

The basemat was analyzed using a three-dimensional finite element ANSYS model of the basemat and attached superstructure. The model extended to elevation 100′ for the auxiliary building and to elevation 236′-0″ for the shield building. Some of the shear walls on the north side were modeled to their full height. The model considered the interaction of the basemat with the overlying structures and with the soil. Two possible uplifts were considered - uplift of the containment internal structures from the lower basemat and uplift of the basemat from the soil.

The vertical stiffness of the soil was represented by a subgrade modulus representative of the soft-to-medium soil case of 520 kips per cubic foot. The horizontal stiffness was represented by horizontal springs attached to some of the basemat nodes. Reactions on the side walls below grade were conservatively neglected. The containment internal structures were simulated with tetrahedral elements connected to the basemat with spring elements normal to the theoretical surface of the containment vessel.

The analyses considered dead loads, live loads, safe shutdown earthquake and containment pressure loads. Safe shutdown earthquake loads were conservatively applied as equivalent static loads for the soft rock case, in combination with the properties of soft-to-medium soil, since the soft rock case produces higher applied seismic forces to the structure than the soft-to-medium soil case. The safe shutdown earthquake loads were applied as static loads using the assumption that while maximum response occurs from one direction, the responses from the other two directions are 40 percent of the maximum.

Linear analyses were performed for the specified load combinations assuming that the soil springs can take tension. Critical load cases were then selected for non-linear analyses with basemat liftoff based on the results of the linear cases. The results from the analysis included forces, shears, and moments in the basemat, bearing pressures under the basemat, and the area of the basemat that is uplifted. Reinforcing steel areas calculated from the member forces for each load combination case were used for design of the DISH portion below the containment and shield building.

The refinement of the finite element model in some areas of the 6’ thick basemat below the auxiliary building was not considered adequate for design. Hence, the required reinforcing steel for the portion of the basemat under the auxiliary building was calculated from shears and bending moments in the slab obtained from separate calculations using the bearing reactions from the finite element analyses. Beam strip models of the slab segments were loaded with the bearing pressures under the basemat from the three-dimensional finite element analyses. The reinforcement required by these analyses on uniform soil springs was increased such that the basemat can resist loads 20 percent greater. This increase accommodated lateral variability of the soil investigated separately in a series of parametric studies described below.

The design of two critical bays of the basemat was described in subsection 3.8.5.4.3:

- Basemat between column lines 9.1 and 11 and column lines K and L
- Basemat between column lines 1 and 2 and column lines K-2 and N

A series of parametric analyses were performed to investigate the assumptions of a uniform subgrade modulus used as the design basis for the nuclear island basemat as described in the previous subsection.

- The three-dimensional finite element model had a subgrade modulus (520 kips per cubic foot) corresponding to a soft-to-medium soil. A parametric study was performed that indicated soft-to-medium soil resulted in higher shears and bending moments in the basemat than stiffer soils or rock.

- The three-dimensional finite element model used a uniform soil stiffness (520 kips per cubic foot) over the entire nuclear island foundation. Parametric studies were performed using a simplified model for two other soil stiffness variations. One variation considered the subgrade modulus equal to 1200 kips per cubic foot at the exterior walls and varied linearly to 400 kips per cubic foot at the center of the basemat. The other global variation considered 400 kips per cubic foot at the edges and varied linearly to 1200 kips per cubic foot at the center. Shear forces and bending moments in the exterior bay of the basemat were compared against the design shear forces and bending moments which were calculated by applying the maximum bearing pressure from the uniform soil case to a slab spanning in one direction. Neither of these cases resulted in higher shears nor bending moments than those from the uniform stiffness of soft-to-medium soil.

- Local variation of soil stiffness was considered. A buried rock pinnacle was considered at a soft-to-medium soil site and the increase in reactive soil pressure was estimated using linear elastic models. The analysis indicated that the increase in soil pressure was less than 15 percent for 15 feet of cover and less than 5 percent with 20 feet.

- Lateral variation of soil stiffness was evaluated using a rigid basemat model on soil springs. The AP600 was represented by an equivalent rectangular basemat. Bearing reactions for cases with lateral variation of the subgrade modulus were compared against the bearing reactions at the same locations for the same loading on a uniform subgrade modulus. These investigations showed that lateral soil variability which would be identified during the site investigation does not affect the bearing reactions by more than 20 percent unless the lateral variability is fairly extreme.

2.2.2 AP600 analyses of settlement during construction

AP600 DCD subsection 3.8.5.4.3 describes the analyses of settlement during construction. Construction loads were evaluated in the design of the nuclear island basemat. This evaluation was performed for soil sites meeting the site interface requirements at which settlement is predicted to be maximum. In the expected basemat construction sequence, concrete for the mat is placed in a single placement. Construction continues with a portion of the shield building foundation and containment internal structure and the walls of the auxiliary building. The critical location for shear and moment in the basemat is around the perimeter of the shield building. Once the shield building and auxiliary building walls are completed to elevation 82′ 6″, the load path changes and loads are resisted by the basemat stiffened by the shear walls.

The analyses of settlement for the AP600 were similar to those described in section 2.5 for the AP1000.

2.2.3 AP600 design for lateral earth pressure

AP600 DCD Appendix 2C describes the seismic lateral earth pressures used to design the exterior walls of the AP600. The loads were based on 2D SASSI analyses that considered interaction between the nuclear island and the adjacent buildings. The lateral earth pressures obtained from SASSI were adjusted to consider the effect of torsional motion of the nuclear island and to consider the local distribution at the corners of the nuclear island.

2.2.4 AP600 nuclear island stability

AP600 DCD subsection 3.8.5.5 describes the evaluation of the minimum factors of safety against sliding, overturning, and flotation for the AP600 nuclear island structures.

The sliding resistance is based on the maximum soil passive pressure resistance and the friction force developed between the basemat and the foundation using a coefficient of friction of 0.55.

The factor of safety against overturning of the nuclear island during a safe shutdown earthquake is evaluated using the static moment balance approach assuming overturning about the edge of the nuclear island at the bottom of the basemat. The resisting moment is equal to the nuclear island dead weight, minus maximum safe shutdown earthquake vertical force and buoyant force from ground water table, multiplied by the distance from the edge of the nuclear island to its center of gravity.

2.3 AP1000 certified design for hard rock sites

2.3.1 AP1000 basemat analyses and design

The analysis and design of the AP1000 nuclear island basemat generally followed the methodology previously described in section 2.2.1 for the AP600. Only differences from the AP600 analyses are described below.

The three-dimensional finite element model of the basemat included all of the nuclear island structures. The finite element model of the basemat is more refined than that used for the AP600 and had sufficient refinement that the member forces from the ANSYS analyses were used directly for the design of the reinforcement, thus eliminating the separate hand calculations using bearing pressure.

The subgrade modulus used in the analyses for hard rock was 6263 kips per cubic foot instead the 520 kips per cubic foot used for the AP600 soft to medium soil case.

In the AP600 design certification, soil bearing requirements were specified only under static loads. For the AP1000 the static demand increased 7.5% due primarily to the increase in height of the shield building. For AP1000 a requirement was added for dynamic loads. The value of 120,000 lb/ft^2 was based on the maximum bearing reaction from the equivalent static non-linear nuclear island basemat analyses described in subsection 3.8.5. This maximum bearing reaction occurs below the west edge of the thick concrete basemat below the shield building. This value was included in DCD Table 2-1 since it was expected that a hard rock site would provide adequate bearing.

2.3.2 AP1000 analyses of settlement during construction

Settlement at a hard rock site is small and is not significant to the design of the AP1000. No analyses were performed for the hard rock site.

2.3.3 AP1000 design for lateral earth pressure

The exterior walls of the seismic Category I structures below the grade are designed to resist the worst case lateral earth pressure loads (static and dynamic), soil surcharge loads, and loads due to external flooding. The lateral earth pressure loads are evaluated for two cases:

- Lateral earth pressure equal to the sum of the static earth pressure plus the dynamic earth pressure calculated in accordance with ASCE 4-98 (Reference 5), Section 3.5.3, Figure 3.5-1, "Variation of Normal Dynamic Soil Pressures for the Elastic Solution"

- Lateral earth pressure equal to the passive earth pressure

2.3.4 AP1000 nuclear island stability

AP1000 DCD subsection 3.8.5.5 describes the evaluation of the minimum factors of safety against sliding, overturning, and flotation for the AP1000 nuclear island structures. The methodology is similar to that described in subsection 2.2.4 for the AP600. Maximum base shear and overturning moments were taken from the time history analyses of the nuclear island lumped mass stick model.

2.4 Analyses of AP1000 foundation response on hard rock and soil sites

This section describes dynamic analyses of the nuclear island and the bearing reactions on the underside of the basemat. The assumptions in the analyses are described and the soil bearing reactions are discussed. The requirement for site bearing is determined from these analyses.

2.4.1 2D SASSI analyses

Parametric 2D SASSI linear elastic analyses were performed for a variety of soil conditions as described in Section 4.4.1.2 of Reference 3. The SASSI model in the east west direction is shown in Figures 2.4-1 and 2.4-2. These analyses used AP1000 building models comprising 3 sticks (ASB, CIS and SCV). Six soil cases with shear wave velocity profiles shown in Figure 2.4-3 were analyzed in each horizontal direction. Bedrock with shear wave velocity of 8000 fps was assumed at a depth of 120' below grade. Thus the depth of soil below the foundation mat is 80.5'. The building models used in the parametric analyses were updated to include changes to the nuclear island such as the change to the enhanced shield building. The properties of the ASB and CIS in the NI combined stick model are developed to match the properties of the nuclear island shell models.

Bending moments in the building sticks for the six AP1000 cases are shown in Figure 4.4.1-5 of Reference 3. The ASB and CIS sticks are coupled below grade. The bending moments in the ASB stick above grade are shown in Table 2.4-1 from the analyses of the updated model. These bending moments provide a direct measure of the effect of soils on the total overturning moment. These overturning moments lead to the maximum bearing pressures which control design of the basemat and the demand on the soil.

Table 2.4-2 shows the reactions at the underside of the basemat for each soil case. These are conservative estimates using the results of the 2D SASSI analyses also used for the member forces in Table 2.4-1. Horizontal loads on the portion below grade are added absolutely to the sum of the member forces above grade. The 2D SASSI reactions (Fx, Fy, and Fz) are used to obtain seismic response factors between the hard rock case to the upper-bound-soft-to-medium (UBSM) soil case, and the soft-to-medium (SM) soil case. These factors were used to adjust the hard rock base reaction time history to reflect the seismic response for the other two potential governing soil cases UBSM and SM.

The soft-to-medium soil case and the upper bound soft to medium soil case result in the largest bending moments in the ASB stick at grade for seismic input in the east west direction. The AP1000 footprint is shorter along the east west axis than along the north south axis. Softer sites typically have lower soil strength than the firmer sites. From review of the member forces in Table 2.4-1, and the bearing reactions in Table 2.4-2, the soft to medium soil case and the upper bound soft to medium soil case are selected as the basis for the bearing demand. The effect of lift off is investigated for these cases as described in the following section. The hard rock case was also analyzed since this case had been included in the hard rock design certification.

2.4.2 2D ANSYS non-linear dynamic analyses

The SASSI analyses described in section 2.4.1 are linear elastic analyses. They permit tension to be carried across the interface between the soil and the basemat. Dead and live load bearing pressures from the ANSYS analyses on soil springs are shown in Figure 2.6-3. The bearing pressures vary from about 6 ksf on the east side to 14 ksf below the edge of the shield building on the west side. The absolute value of some of the seismic bearing pressures calculated by SASSI exceed the dead load bearing pressures giving a resultant tension uplift. The effect of lift off was analyzed in ANSYS. Linear seismic analyses were performed on the ANSYS models to confirm similar behavior to the SASSI analyses. Non-linear analyses were then performed for dead plus seismic loads with compression only contact elements.

Lift off was evaluated using an East-West lumped-mass stick model of the nuclear island structures supported on a rigid basemat with nonlinear springs. The liftoff analysis model is shown in Figure 2.4-4 and consists of the following elements:

- The nuclear island (NI) combined stick model (ASB, CIS and SCV). The three sticks are concentric and the reactor coolant loop is included as mass only. This model is the same model as was used in the updated 2D SASSI analyses described in Section 2.4.1.
- The rock and soil were modeled as horizontal and vertical spring elements with viscous damping at each node of the rigid beam. The vertical soil spring at each node is the subgrade modulus shown in Table 2.4-3 multiplied by the area of the footprint associated with each node. The horizontal spring is calculated from that in the vertical direction assuming that the ratio of horizontal and vertical stiffness for the layered site has the same relationship as for a semi-infinite medium. Soil damping is included in the soil spring element and is calculated to give the percentage shown in Table 2.4-3 at the fundamental frequency of the building soil system.
- The rigid basemat model with a footprint area that varies along the East-West (Y) axis of the model matching the footprint of the nuclear island. The NI combined stick is attached to the rigid basemat at the NI gravity center, which is about 9 feet from the center of the rigid basemat. In the north-south direction, the stick is fixed at the bottom (EL. 60.5').

Direct integration time history analyses were performed. Time histories were applied at the underside of the foundation (elevation 60.5'). These time histories were foundation level inputs calculated from the AP1000 time histories at grade using a SHAKE analysis with the degraded properties shown in Figure 2.4-3(b). Structural damping was included as mass and stiffness proportional Rayleigh damping matching the modal damping of 7% at the fundamental frequency and at 25 Hertz. The first ANSYS analyses used Rayleigh damping matching 7%. Floor Response Spectra (FRS) and member force results were compared to those from 2D SASSI. The bending moment on the Auxiliary Shield Building (ASB) stick at grade is used as a measure of the overturning which is of greatest significance in the lift off analyses. The SASSI and ANSYS results showed the largest overturning for the UBSM and SM soil cases. For these soil cases the ANSYS results of both the FRS and member forces were lower than the SASSI results. The Rayleigh damping was reduced from 7% to 5 % for UBSM and SM so that the FRS and ASB bending moment at grade matched those from SASSI. Typical FRS are compared in Figure 2.4-5 for the soft to medium soil case. In the horizontal direction the FRS compare very well. In the vertical direction the ANSYS analyses show higher values than SASSI making the ANSYS analyses slightly more conservative; this is partially due to the Rayleigh damping which is selected to give appropriate damping for the horizontal frequency around 2.5 Hz and gives much lower damping at the fundamental vertical frequency of about 6 Hz. The ASB bending moments at grade are compared in Table 2.4-4. These show a good match between the ANSYS and SASSI models.

Time history analyses were run by direct integration for dead load plus the east west and vertical components of the safe shutdown earthquake for two cases:

- linear soil springs able to take both tension and compression. This case was run to compare against the linear results from the 2D SASSI analyses to confirm the soil springs and damping properties.
- non-linear soil springs where the vertical springs act in compression only and the horizontal springs are active when the vertical spring is closed and inactive when the vertical spring lifts off.

Comparisons of floor response spectra for these two cases show that the liftoff has insignificant effect on the SSE floor response spectra. Thus, the superstructure may be designed neglecting liftoff. Only the basemat design need consider the effects of liftoff as described in Section 2.6.

Figure 2.4-6 shows the time history of the deflection and pressure at the west and east edge around the time that the peak pressure occurs at the west edge. The three sheets show results for hard rock (HR), upper bound soft to medium (UBSM) and soft to medium (SM). The linear results show maximum bearing pressures on the west side of 31 to 33 ksf. Lift off increases the subgrade pressure close to the west edge by 4 to 6% with insignificant effect beneath most of the basemat. The effect on the pressure at the west edge is significantly less than that calculated in the non-linear basemat analyses using equivalent static accelerations.

2.4.3 3D SASSI Analyses

The SASSI Soil-Structure Interaction analyses are performed based on the Nuclear Island 3D SASSI Model for the hard rock and five soil conditions established from the AP1000 2D SASSI analyses. The SASSI Model of Nuclear Island is based on the NI20 Coarse Finite Element (described in Reference 3). The detailed 3D SASSI analysis is described in Section 4.4.2 of Reference 3.

2.4.4 Site interface for soil

The bearing pressures from the 3D SASSI analyses have been obtained by combining the time history results from the North-South, East-West, and vertical earthquakes. The maximum bearing pressures obtained from the various soil cases are listed in Table 2.4-5.

The AP1000 requirements are as follows:

Soil	
Average Allowable Static Bearing Capacity	Greater than or equal to 8,900 lb/ft^2 over the footprint of the nuclear island at its excavation depth
Dynamic Bearing Capacity for Normal Plus SSE	Greater than or equal to 35,000 lb/ft^2 at the edge of the nuclear island at its excavation depth or,

Site specific analyses demonstrate factor of safety appropriate for normal plus safe shutdown earthquake loads.

In the AP600 design certification, soil bearing requirements were specified only under static loads. For the AP1000 the static demand increased 7.5% due primarily to the increase in height of the shield building. The AP1000 DCD for hard rock added a requirement of 120,000 lb/ft^2 for dynamic loads. This was based conservatively on the maximum bearing reaction from the equivalent static non-linear nuclear island basemat analyses described in section 2.3. This maximum bearing reaction occurs below the west edge of the thick concrete basemat below the shield building. This value was included in DCD Table 2-1 since it was expected that a hard rock site would be capable of satisfying this bearing demand. The dynamic non-linear analyses described in section 2.4.2 show much lower bearing reactions (27.8 ksf for hard rock) than those from the equivalent static design analyses for the basemat. The 2D ANSYS non-linear analyses show that the soft-to-medium soil case gives higher bearing pressures (34.5 ksf) than the hard rock case. This establishes the soil bearing interface of 35,000 lb/ft^2. The bearing pressures from the ANSYS analyses are conservative because the effect of the side soil is conservatively neglected.

Limitations on soil variability were included in DCD Rev 17 Table 2-1. These limitations are applicable to foundation design.

Table 2.4-1

Maximum member forces in ASB stick at elevation 99' from 2D SASSI analyses

Units: 1000 kips & 1000 ft-kip

	North-South model		**East-West model**	
Soil case	**North-South Shear**	**Moment about E-W axis**	**East-West Shear**	**Moment about N-S axis**
	F_X	M_{YY}	F_Y	M_{XX}
Hard Rock (HR)	52.85	6934	46.77	6085
Firm Rock (FR)	49.81	6837	48.05	6118
Soft Rock (SR)	50.54	6586	51.58	6554
Upper Bound Soft to Medium Soil (UBSM)	52.12	6416	55.24	7084
Soft to Medium Soil (SM)	53.24	6810	61.67	7621
Soft Soil (SS)	26.01	3683	28.08	4649

Table 2.4-2 – Maximum Seismic Reactions at Center Line of Containment

Units: 1000 kips & 1000 ft-kip

Seismic Reactions	**HR**	**FR**	**SR**	**UBSM**	**SM**	**SS**
Shear NS, F_X	123.75	116.49	118.65	121.48	113.61	73.11
Shear EW, F_Y	112.31	113.55	121.88	128.11	124.94	74.34
Vertical, F_Z	98.76	98.65	99.63	104.55	112.30	94.48
Moments Relative to Centerline of Containment						
M_{XX} EW Excitation	10,916	10,900	11,471	12,229	12,607	7,653
M_{XX} Vertical Excitation	1,660	1,693	1,715	2,017	1,913	1,459
M_{XX} SRSS	11,042	11,031	11,598	12,394	12,751	7,791
M_{YY} NS Excitation	12,184	11,659	11,390	11,274	11,173	6,300
M_{YY} Vertical Excitation	918	935	946	997	1,059	829
M_{YY} SRSS	12,218	11,697	11,429	11,318	11,223	6,354

Notes:

1. HR = Hard Rock, FR = Firm Rock, SR = Soft Rock, UBSM = Upper Bound Soft to Medium Soil, SM = Soft to Medium Soil, SS = Soft Soil.
2. Reactions for horizontal input are calculated from member forces at grade in 2D SASSI analyses plus maximum acceleration times mass below grade. Reactions due to vertical input are calculated from maximum accelerations in 3D ANSYS or SASSI analyses for HR, FR, UBSM and SM and from 2D ANSYS analyses for SR and SS.

Table 2.4-3

Soil Properties in ANSYS Model

Soil case	Assumption of Soil Conditions				
	Soil Material Property		ANSYS Soil Spring Property		
	Density pcf	**Poisson's Ratio**	**Stiffness** kcf		**Damping** %
			Vertical	**East-West**	
Hard Rock	150	0.250	6300	5477	2
Firm Rock	150	0.250	2800	2434	5
Soft Rock	150	0.250	1700	1478	5
Upper Bound Soft to Medium Soil	110	0.35 / 0.383 (2)	1500	1187	5
Soft to Medium Soil	110	0.35 / 0.450 (2)	900	666	5
Soft Soil	110	0.40 / 0.483 (2)	300	213	20

Notes:

1. Soil conditions are identified using the same notation as in Reference 3.
2. Poisson's ratio is shown for dry soils. The second value is the average value over the depth of the soil column accounting for ground water. This value is used in establishing horizontal springs.
3. Soil spring damping is applied as damping element to give specified damping at the first frequency.

Table 2.4-4

Comparison of member forces in ASB stick at elevation 99' from 2D SASSI and ANSYS analyses

Units: 1000 kips & 1000 ft-kip

	SASSI			ANSYS		
Soil case	**Axial**	**East-West Shear**	**Moment about N-S axis**	**Axial**	**East-West Shear**	**Moment about N-S axis**
	F_Z	F_Y	M_{XX}	F_Z	F_Y	M_{XX}
Hard Rock (HR)	47.72	46.77	6085	52.95	52.01	6330
Firm Rock (FR)	48.67	48.05	6118	54.78	53.84	6428
Soft Rock (SR)	49.48	51.58	6554	57.34	53.68	6592
Upper Bound Soft to Medium Soil (UBSM)	52.20	55.24	7084	61.14	60.18	7581
Soft to Medium Soil (SM)	54.78	61.67	7621	63.80	58.65	7311
Soft Soil (SS)	37.96	28.08	4649	52.39	32.63	4009

Table 2.4-5
SASSI 3D Maximum Bearing Pressure

Soil Case	Pressure (Ksf)
Hard Rock (No side soil)	35.0*
Firm Rock	27.9
Soft Rock	24.0
Upper Bound Soft to Medium	25.7
Soft to Medium	23.1
Soft Soil	21.9

Notes:
* 38.3 ksf was the maximum localized peak calculated; a limit of 35 ksf for maximum bearing seismic demand is obtained by averaging the soil pressure about the West edge of the shield building where the maximum stress occurs.

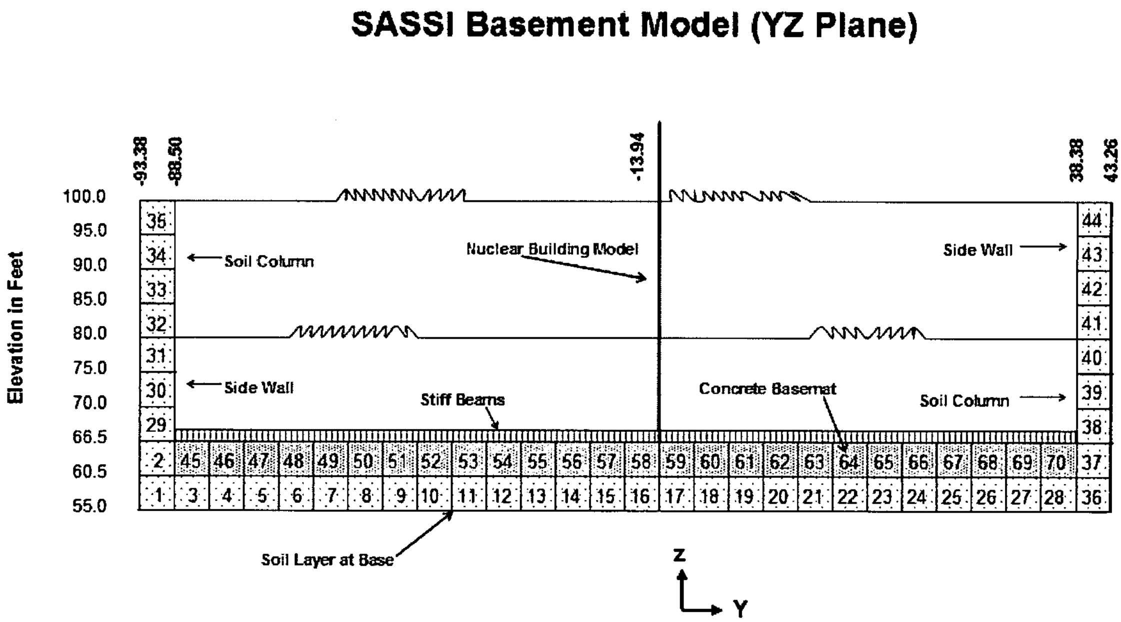

Figure 2.4-1: SASSI Basement Model (YZ Plane)

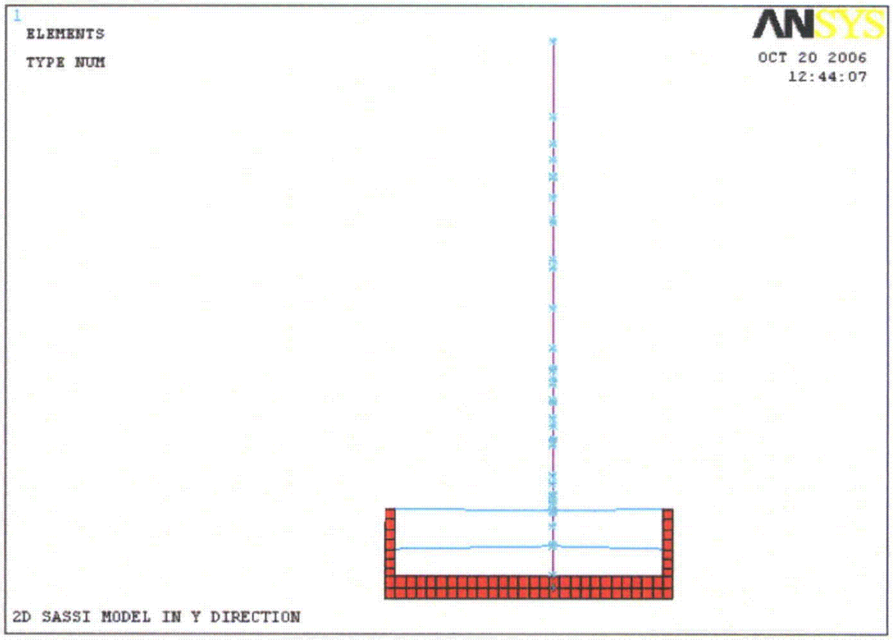

Figure 2.4-2: East-West 2D SASSI Model in Y Direction

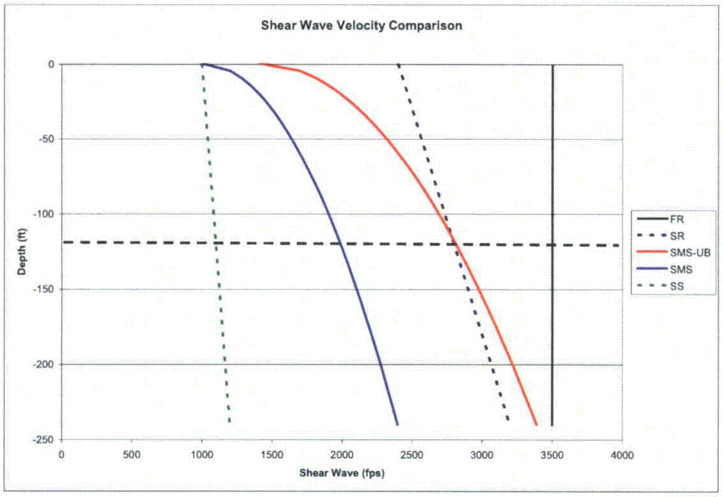

a) Low strain values

Notes:

Fixed base analyses were performed for hard rock sites. These analyses are applicable for shear wave velocity greater than 8000 feet per second.
Design analyses have soil to depth of 120' with rock below having shear wave velocity of 8000 feet per second.

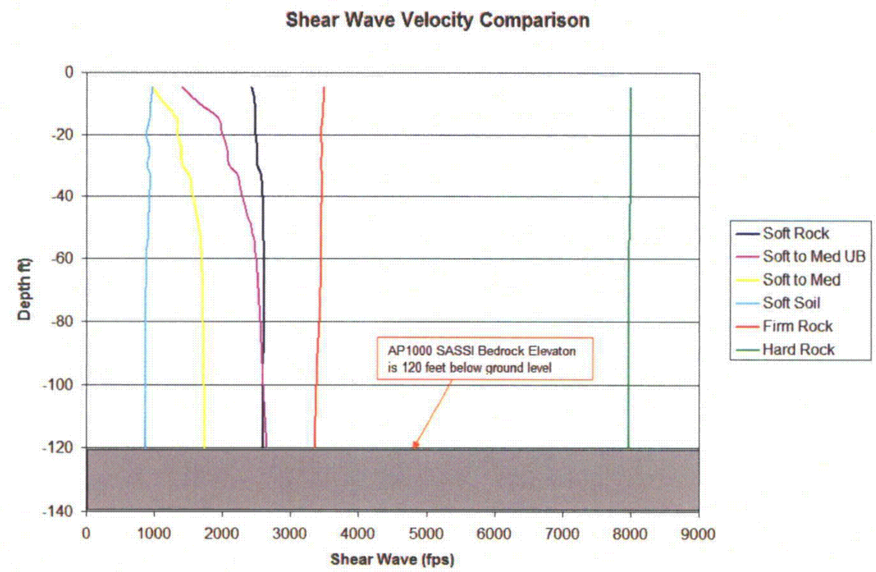

b) Degraded values for SSE analyses

Figure 2.4-3 Generic Soil Profiles

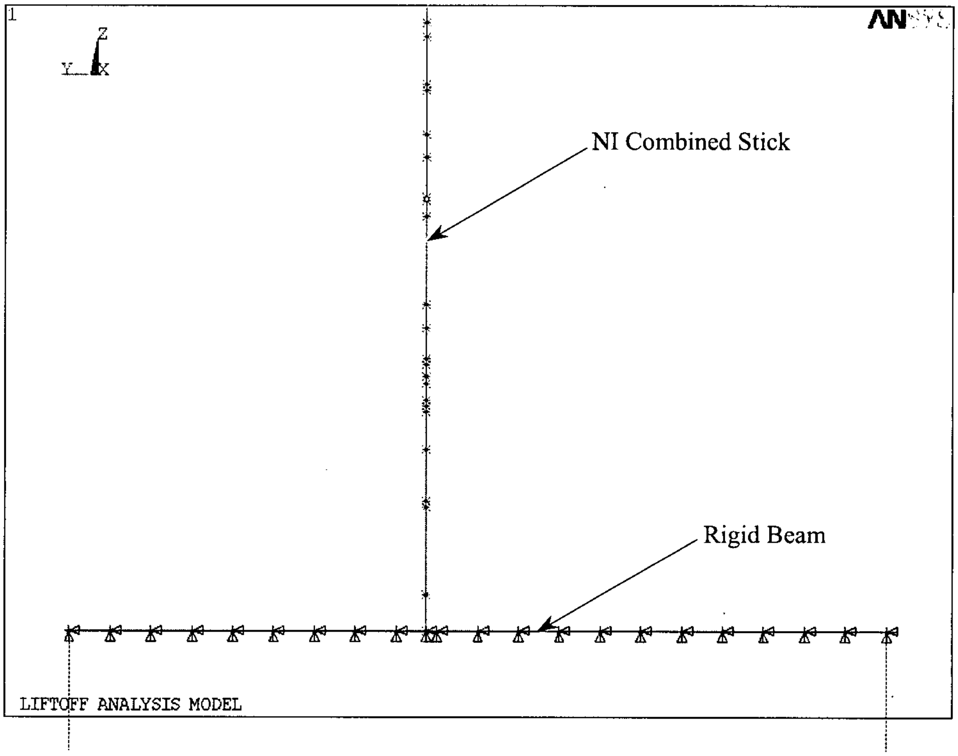

Figure 2.4-4 – ANSYS Lift Off Model

<table>
<tr><th>Horizontal</th><th>Vertical</th></tr>
<tr><td colspan="2">ASB - Top of Shield Building – Elevation 327’</td></tr>
<tr><td>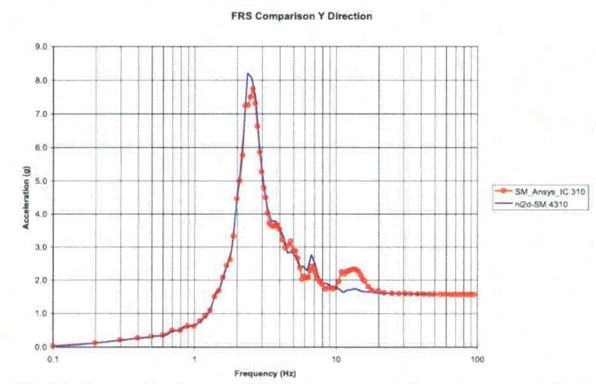
</td><td>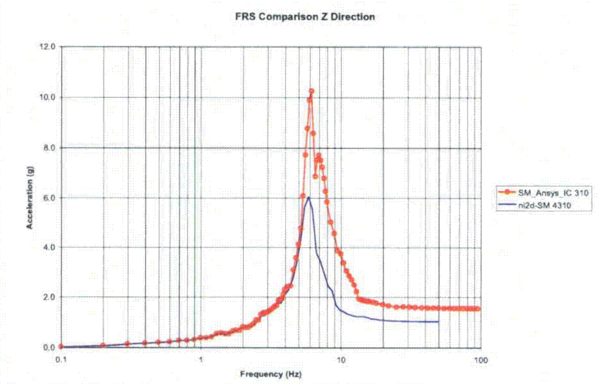
</td></tr>
<tr><td colspan="2">ASB - Top of Fuel Building – Elevation 180’</td></tr>
<tr><td>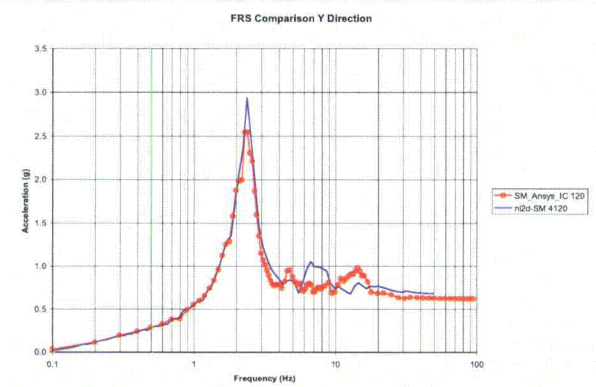
</td><td>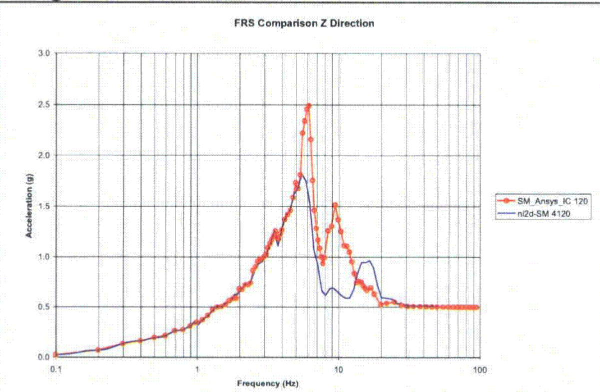
</td></tr>
<tr><td colspan="2">ASB Elevation 99’</td></tr>
<tr><td>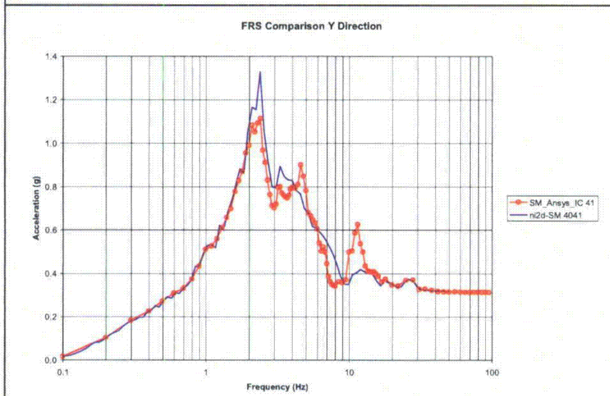
</td><td>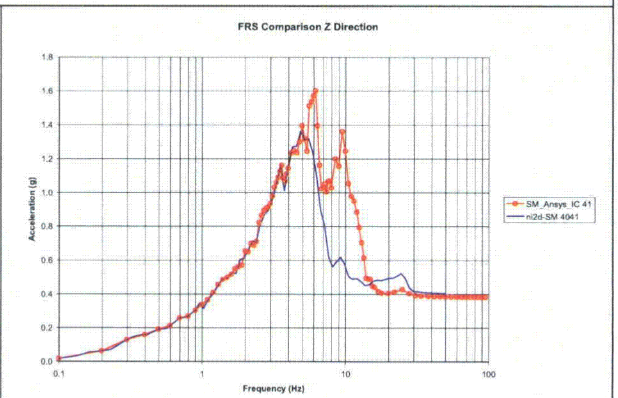
</td></tr>
</table>

Figure 2.4-5 Comparison of SASSI and ANSYS FRS for Soft to Medium Soil

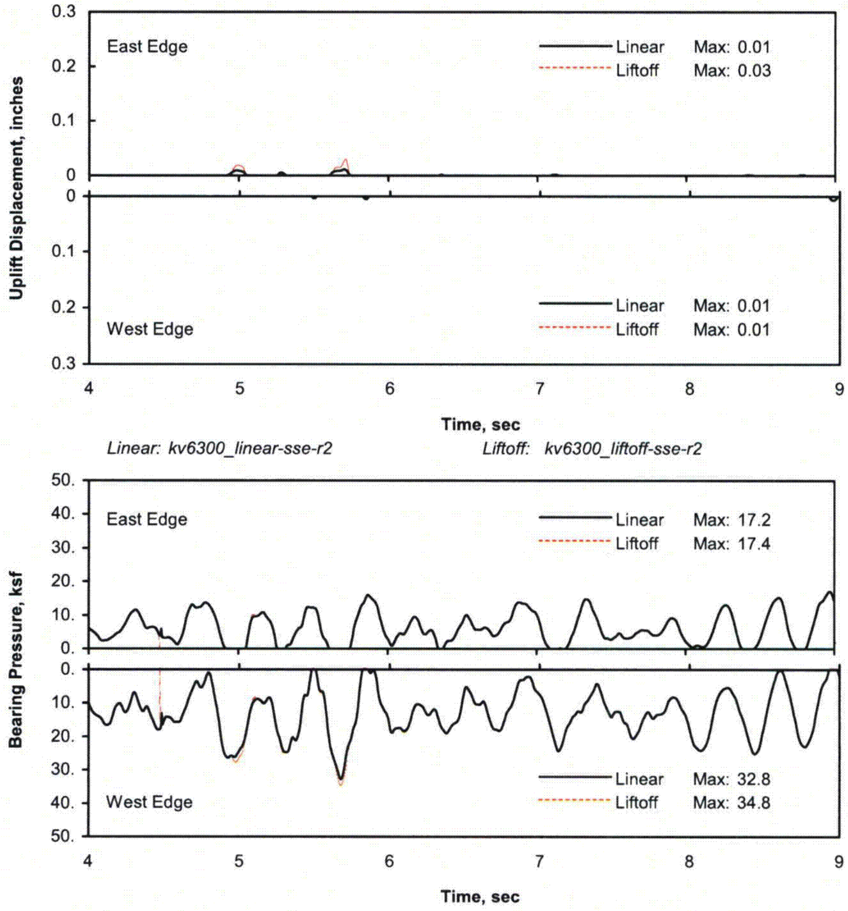

Maximum uplift Displacements					
East			West		
	inches	Time(s)		inches	Time(s)
Linear	0.01	5.71	Linear	0.01	8.94
Liftoff	0.03	5.72	Liftoff	0.01	8.96

Maximum Bearing Pressure					
East			West		
	ksf	Time(s)		ksf	Time(s)
Linear	17.18	8.97	Linear	32.77	5.68
Liftoff	17.38	8.97	Liftoff	34.85	5.68

Figure 2.4-6 – 2D ANSYS Time History of Basemat Edges

Sheet 1 of 3 –Hard Rock Case

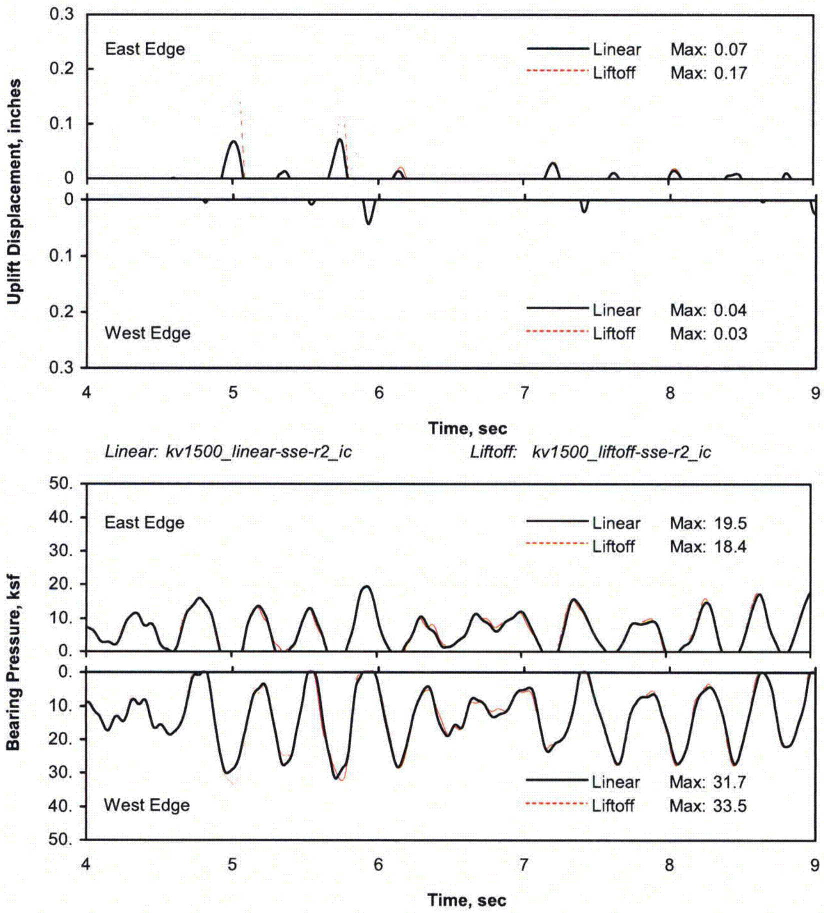

Maximum uplift Displacements					
East			West		
	inches	Time(s)		inches	Time(s)
Linear	0.07	5.74	Linear	0.04	5.92
Liftoff	0.17	5.03	Liftoff	0.03	9.00

Maximum Bearing Pressure					
East			West		
	ksf	Time(s)		ksf	Time(s)
Linear	19.46	5.93	Linear	31.69	5.71
Liftoff	18.42	5.90	Liftoff	33.51	5.01

Figure 2.4-6 2D ANSYS Time History of Basemat Edges

Sheet 2 of 3 –Upper-Bound Soft-to-Medium Soil

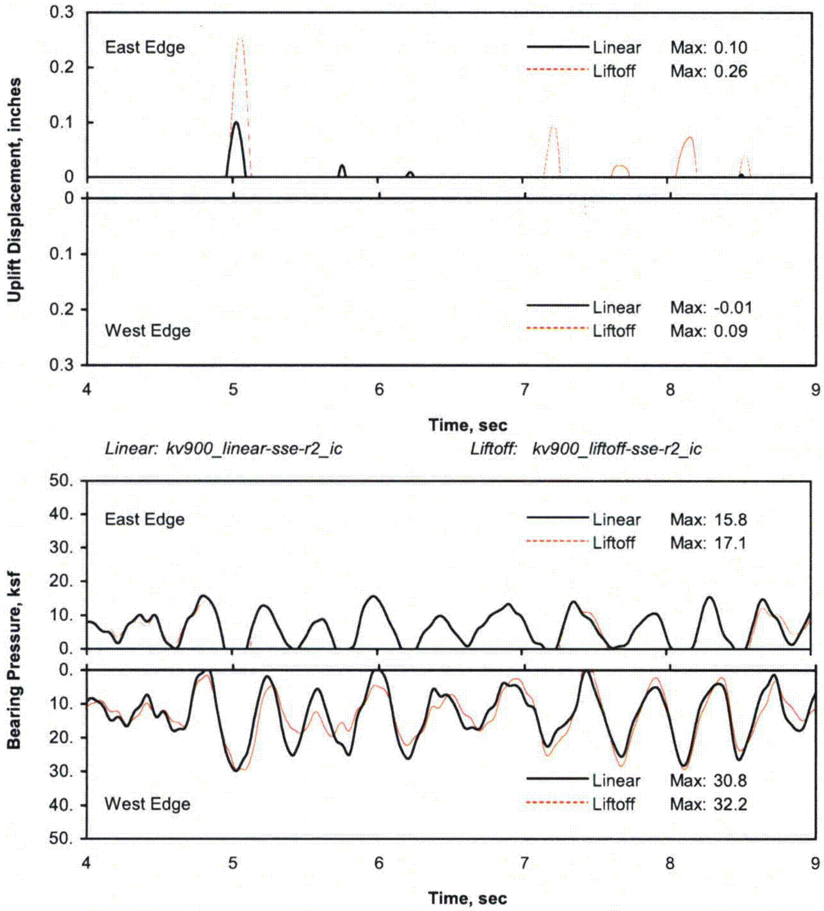

Maximum uplift Displacements					
East			West		
	inches	Time(s)		inches	Time(s)
Linear	0.10	5.03	Linear	-0.01	10.81
Liftoff	0.26	5.06	Liftoff	0.09	10.85

Maximum Bearing Pressure					
East			West		
	ksf	Time(s)		ksf	Time(s)
Linear	15.84	4.80	Linear	30.82	10.60
Liftoff	17.06	10.41	Liftoff	32.18	10.61

Figure 2.4-6 2D ANSYS Time History of Basemat Edges

Sheet 3 of 3 –Soft-to-Medium Soil

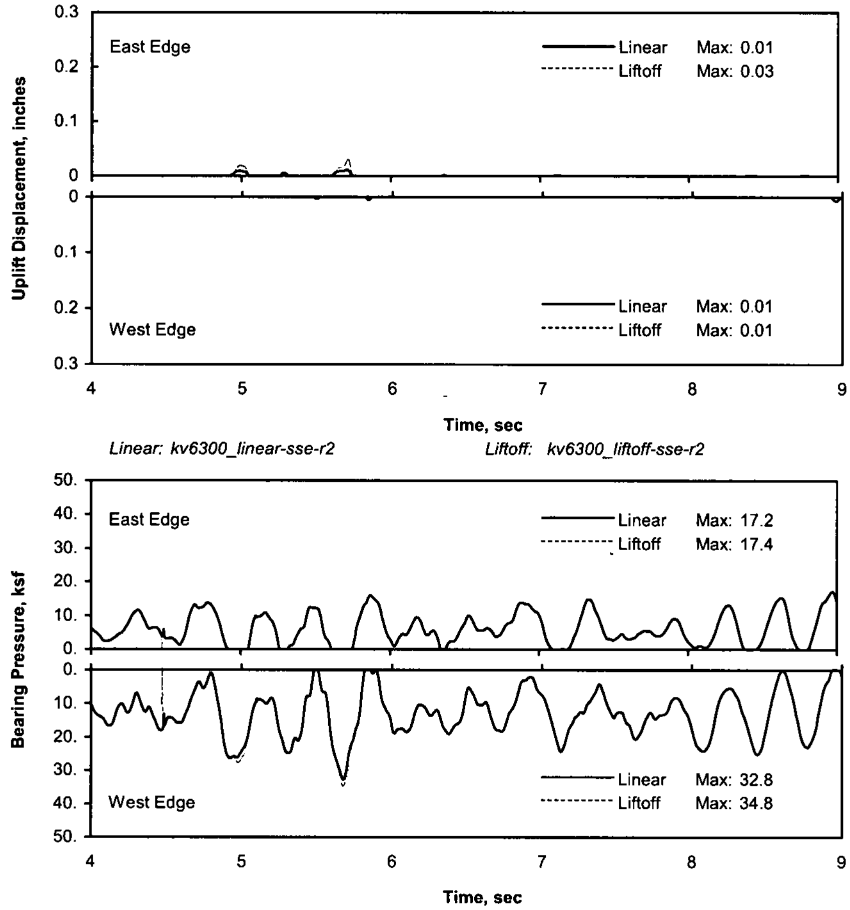

Maximum uplift Displacements					
East			West		
	inches	Time(s)		inches	Time(s)
Linear	0.01	5.71	Linear	0.01	8.94
Liftoff	0.03	5.72	Liftoff	0.01	8.96

Maximum Bearing Pressure					
East			West		
	ksf	Time(s)		ksf	Time(s)
Linear	17.18	8.97	Linear	32.77	5.68
Liftoff	17.38	8.97	Liftoff	34.85	5.68

Figure 2.4-6 – 2D ANSYS Time History of Basemat Edges

Sheet 1 of 3 –Hard Rock Case

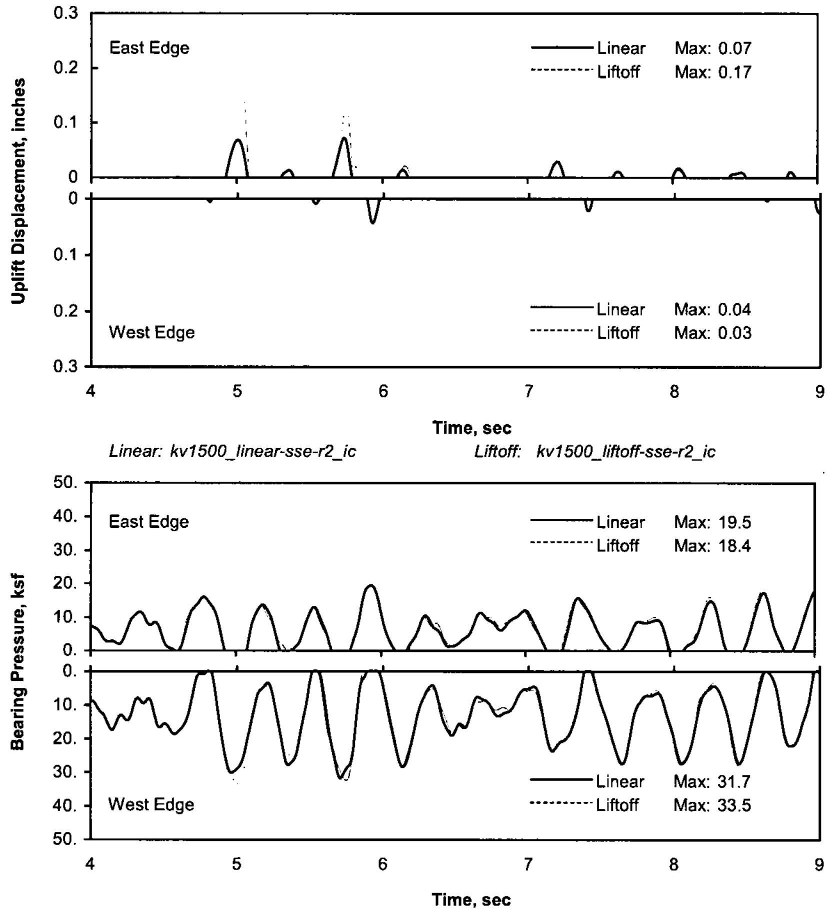

Maximum uplift Displacements					
East			West		
	inches	Time(s)		inches	Time(s)
Linear	0.07	5.74	Linear	0.04	5.92
Liftoff	0.17	5.03	Liftoff	0.03	9.00

Maximum Bearing Pressure					
East			West		
	ksf	Time(s)		ksf	Time(s)
Linear	19.46	5.93	Linear	31.69	5.71
Liftoff	18.42	5.90	Liftoff	33.51	5.01

Figure 2.4-6 2D ANSYS Time History of Basemat Edges

Sheet 2 of 3 –Upper-Bound Soft-to-Medium Soil

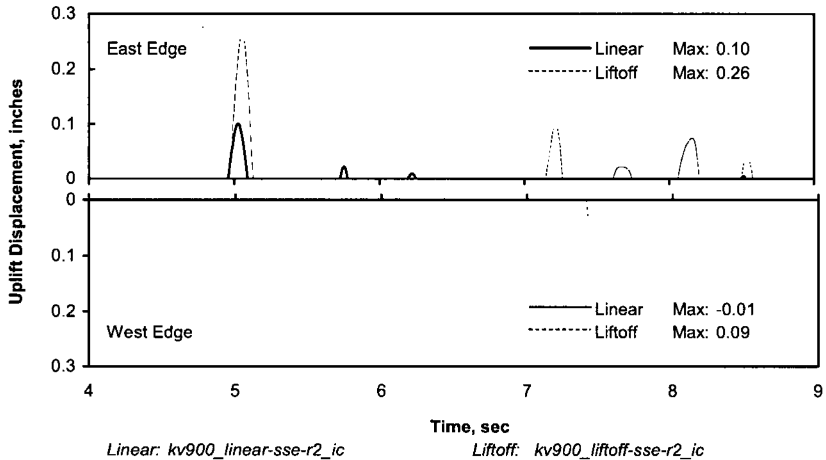

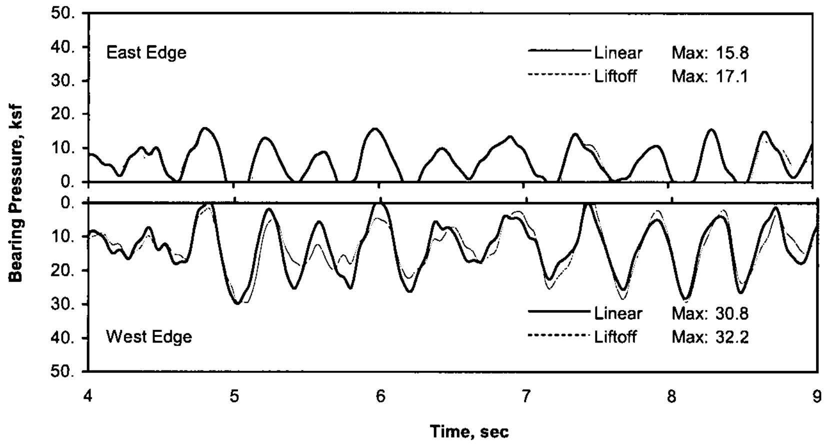

Maximum uplift Displacements					
East			West		
	inches	Time(s)		inches	Time(s)
Linear	0.10	5.03	Linear	-0.01	10.81
Liftoff	0.26	5.06	Liftoff	0.09	10.85

Maximum Bearing Pressure					
East			West		
	ksf	Time(s)		ksf	Time(s)
Linear	15.84	4.80	Linear	30.82	10.60
Liftoff	17.06	10.41	Liftoff	32.18	10.61

Figure 2.4-6 2D ANSYS Time History of Basemat Edges

Sheet 3 of 3 –Soft-to-Medium Soil

2.5 Analyses of settlement during construction

Construction loads were evaluated in the design of the nuclear island basemat. This evaluation was performed for soil sites meeting the site interface requirements at which settlement is predicted to be maximum. In the expected basemat construction sequence, concrete for the mat is placed in a single placement. Construction continues with a portion of the shield building foundation and containment internal structure and the walls of the auxiliary building. The critical location for shear and moment in the basemat is around the perimeter of the shield building. Once the shield building and auxiliary building walls are completed to elevation 82′ -6″, the load path changes and loads are resisted by the basemat stiffened by the shear walls.

The analyses account for the construction sequence, the associated time varying load and stiffness of the nuclear island structures, and the resulting settlement time history. To maximize the potential settlement, the analyses consider a 360 feet deep soft soil site with soil properties consistent with the soft soil case. Two soil profiles were analyzed to represent limiting foundation conditions, and address both cohesive and cohesionless soils and combinations thereof:

- A soft soil site with alternating layers of sand and clay. The assumptions in this profile maximize the settlement in the early stages of construction and maximize the impact of dewatering.
- A soft soil site with clay. The assumptions maximize the settlement during the later stages of construction and during plant operation.

The analyses focused on the response of the basemat in the early stages of construction when it could be susceptible to differential loading and deformations. As subsequent construction incorporates concrete shear walls associated with the auxiliary building and the shield building, the structural system significantly strengthens, minimizing the impact of differential settlement. The displacements, and the moments and shear forces induced in the basemat were calculated at various stages in the construction sequence. These member forces were evaluated in accordance with ACI 349. Three construction sequences were examined to demonstrate construction flexibility within broad limits.

- A base construction sequence which assumes no unscheduled delays. The site is dewatered and excavated. Concrete for the basemat is placed in a single pour. Concrete for the exterior walls below grade is placed after the basemat is in place. Exterior and interior walls of the auxiliary building are placed in 16 to 18-foot lifts.
- A delayed shield building case which assumes a delay in the placement of concrete in the shield building while construction continues in the auxiliary building. This bounding case maximizes tension stresses on the top of the basemat. The delayed shield building case assumes thât no additional concrete is placed in the shield building after the pedestal for the containment vessel head is constructed. The analysis incorporates construction in the auxiliary building to elevation 117′-6″ and thereafter assumes that construction is suspended.
- A delayed auxiliary building case which assumes a delay in the construction of the auxiliary building while concrete placement for the shield building continues. This bounding case maximizes tension stresses in the bottom of the basemat. The delayed auxiliary building case assumes that no concrete is placed in the auxiliary building after the basemat is constructed. The analysis incorporates construction in the shield building to elevation 84′-0″ and thereafter assumes that construction is suspended.

For the base construction sequence, the largest basemat moments and shears occur at the interface with the shield building before the connections between the auxiliary building and the shield building are credited. Once the shield building and auxiliary building walls are completed to elevation 82′ -6″, the load path for successive loads changes and the loads are resisted by the basemat stiffened by the shear walls. Dewatering is discontinued once construction reaches grade, resulting in the rebound of the subsurface.

Of the three construction scenarios analyzed, the delayed auxiliary building case results in the largest demand for the bottom reinforcement in the basemat. The delayed shield building results in the largest demand for the top reinforcement in the basemat.

The analyses of alternate construction scenarios showed that member forces in the basemat were acceptable subject to the following limits imposed for soft soil sites on the relative level of construction of the buildings prior to completion of both buildings at elevation 82′ -6″:

- Concrete may not be placed above elevation 84′ -0″ for the shield building or containment internal structure.

- Concrete may not be placed above elevation 117′ -6″ in the auxiliary building.

Member forces in the basemat considering settlement during construction differ from those obtained from the design analyses on uniform elastic soil springs. Although the bearing pressures at the end of construction are similar in the two analyses, the resulting member forces differ due to the progressive changes in structural configuration during construction. The design using the results of the design analyses on uniform elastic soil springs provides sufficient structural strength to resist the specified loads including bearing reactions on the underside of the basemat. The member forces in these analyses are those due to primary externally applied loads and do not consider secondary stresses and strains locked in during early stages of construction. A confirmatory evaluation was performed to demonstrate that the member forces due to design basis loads, including locked-in forces due to construction settlement, remain within the capacity of the section. The evaluation was performed for critical locations which were selected as locations where the effect of locked in member forces were judged to be most significant. The member forces for the load combination of dead load plus safe shutdown earthquake, including the member forces locked-in during various stages of plant construction, were within the design capacity for the critical locations. The evaluation demonstrated that the member forces including locked-in forces calculated by elastic analyses remain within the capacity of the section.

2.6 Nuclear island basemat design

The design of the nuclear island basemat is described in the basemat design summary report prepared in accordance with the guidelines of Standard Review Plan 3.8.4. The design is based on the worst combination of seismic loads and soil properties. Non-linear equivalent static analyses are performed which consider lift off of the basemat from the soil. The analyses use the detailed model of the nuclear island (NI05) shown in Figures 2.6-1, 2.6-2 and 2.6-2 (a) thru (d). The soft-to-medium soil case is considered as described in section 2.4.1. These analyses are similar to those described in section 2.2.1 for the AP600 and in section 2.3.1 for the AP1000 on hard rock. The equivalent static loads are developed from accelerations given by time history analyses of the nuclear island on hard rock and soil sites. No credit is taken in these analyses for the effect of side soils.

The design analyses of the nuclear island basemat were performed with the finite element model of the nuclear island prior to the design changes to enhance the shield building. These changes affected the upper portions of the shield building and did not affect the structure close to the basemat. Member forces in the basemat due to the equivalent static accelerations are therefore valid for the given loads. The adequacy of the equivalent static accelerations is addressed in Section 2.6.1.2.

The 3D ANSYS equivalent static nonlinear finite element model, used to evaluate the basemat and foundation walls, is the NI05 model described in DCD Rev 16 Appendix 3G, subsection 3G.2.3. The NI05 model is a large solid-shell finite element model of the AP1000 nuclear island which combines the ASB solid-shell model described in DCD subsection 3G.2.1.1, and the CIS solid-shell model described in DCD subsection 3G.2.1.2. Dead and seismic loads from the containment vessel and polar crane are applied as loads at elevation 100'. The nominal element size in the ASB portion of this NI05 model is about 4.5 feet so that each wall has four elements for the wall height of about 18 feet between floors. Views of this model are provided in Figures 2.6-1, 2.6-2 and 2.6-2 (a) thru (d).

The nuclear island is modeled using the following shell, solid and spring elements:

- Basemat (6 foot thick portion): SHELL43 elements
- Basemat (DISH): SOLID45 elements
- Containment internal basemat (mass concrete): SOLID45 elements
- Auxiliary building walls and floors: SHELL43 elements
- Containment internal structure walls and floors: SHELL43 elements
- containment shell: SHELL43 elements
- shield building: SHELL43 elements
- Linear springs at CV interface: COMBIN14 elements
- Nonlinear soil springs: COMBIN37 elements

The basemat below the containment vessel (DISH) is modeled with solid elements. There are three elements through the thickness as shown in Figures 2.6-2 (a) and (b). Member forces across a section through the solid elements are calculated along a path using the PATH stress function of ANSYS. The accuracy of member forces using three solid elements was confirmed by comparison of results to those from a shell model.

Soil Spring elements (COMBIN37) are attached on each node on the underside of the basemat. For the 6' thick basemat, the nodes are on the center of the 6' thick basemat shell elements (elevation is EL63'-6" at the center of the 6' thick basemat). For the central basemat (DISH), the nodes are on the bottom of the solid elements (elevation is EL60'-6"). At each node three COMBIN37 springs are attached for NS, EW and vertical directions respectively.

The connection of the ASB portion of the model to the DISH representing the mass concrete below the containment vessel is shown in Figure 2.6-2 (c). The solid model extends to the midplane of the cylindrical wall (radius of 71 feet). The shell elements of the shield building cylindrical wall extend down to the underside of the basemat at elevation 60'- 6". The vertical shell elements have a thickness of 1.5 feet (half the thickness of the wall above) in areas where the shell element forms the surface of the solid elements of the mass concrete. Shell elements from the auxiliary building including the basemat connect to the vertical shell elements which in turn are connected to the solid elements, thus providing rotational continuity.

Figure 2.6-2 (d) shows the locations of nodes on the DISH which interface with the containment vessel shell and the containment internal structure basemat. The bottom head of the containment vessel is modeled by shell elements to permit analyses for containment pressure. Coincident nodes are provided for the DISH, the containment vessel and the containment internal structure basemat. The boundary between the CV and CIS, and the boundary without studs between the CV and DISH are modeled with linear spring elements (COMBIN14) normal to the boundary to transmit normal forces only. The boundary with studs between the CV and DISH is modeled with linear spring elements (COMBIN14) normal and parallel to the boundary. In each analysis the spring forces in the normal spring elements are checked for lift off and spring elements are eliminated if liftoff occurs.

2.6.1 3D ANSYS Equivalent Static Non-Linear Analysis

2.6.1.1 Subgrade modulus

The basemat under the auxiliary building is 6 feet thick and supports a grid work of walls. These walls in turn stiffen the slab by producing relatively short spans, in the range of 3 to 4 times the thickness. The design of the 6' thick portion of the mat is controlled by the maximum bearing pressure under the slab during a seismic event. Maximum bearing pressures occur for the case of maximum overturning moment. Due to the shape of the footprint of the nuclear island seismic loads in the east-west direction give the largest bearing pressures and the greatest potential for lift off.

Table 2.6-1 shows the subgrade modulus calculated for each of the generic soil cases using the Steinbrenner method previously used for the AP600. These calculations used the same degraded shear modulus properties in each layer as used in the SASSI analyses. The subgrade moduli shown in Table 2.6-1 were used in the 2D ANSYS analyses described in section 2.4.2. The subgrade moduli were confirmed by results of an ANSYS study. Floor response spectra from the ANSYS analyses compared well in the frequency range of soil structure interaction to the results of 2D SASSI. These comparisons confirmed that the subgrade moduli provide a close match for the overall dynamic response.

Reinforcement design uses member forces from analyses of the nuclear island on soil springs. The shear and bending moment in the basemat are dependent on the relative stiffness of material supporting the foundation and the global stiffness of the nuclear island buildings and the local bending stiffness of the basemat. The walls of the nuclear island are stiff relative to a soil. The contact pressure is nearly linearly distributed and the actual magnitude of the subgrade modulus has small effect on the member forces in walls of the nuclear island. The local slabs of the basemat, spanning 18 to 25 feet between walls, are flexible relative to the subgrade. For such a case, there will be a decrease in pressure near the center of the slab and an increase in pressure near the walls. This redistribution decreases as the subgrade modulus decreases. It is therefore conservative for the design of the basemat to use a low value of the subgrade modulus. This is discussed further in section 2.7 which describes analyses of a detailed model of portions of the basemat on both soil springs and soil finite elements.

The AP600 basemat analysis used the soft to medium linear profile (this profile was subsequently changed to the parabolic profile thus increasing shear wave velocity below the nuclear island). Soil springs of 520 kcf were established by the Steinbrenner method using undegraded properties and soil up to grade.

Although the subgrade modulus calculated for the AP1000 soil cases in Table 2.6-1 could have justified use of a subgrade modulus of 578 kcf for the dry soft to medium soil or 963 kcf with the water table above the foundation level, it was decided to retain the 520 kcf used in the AP600 analyses. As described above this is conservative since it maximizes the bending moments in the slabs. It also permitted a direct comparison of the AP1000 analyses to those for the AP600.

2.6.1.2 Equivalent static accelerations

Seismic loads for the evaluation of the basemat of the Nuclear Island were developed from the results of the global seismic analyses on hard rock using models prior to the design change to enhance the shield building. They are specified as equivalent static seismic accelerations as shown in Table 2.6-2(a).

The equivalent static accelerations used in the non-linear design analyses of the nuclear island basemat were evaluated for the revised design with the enhanced shield building by comparing total base reactions and bearing pressures in a linear analysis using these equivalent static accelerations to those from a dynamic analysis of the updated nuclear island model (NI20). A time history fixed base analysis of the updated model was performed using time history inputs that envelope the basemat response given by the 3D SASSI analyses at the corners and centers of the basemat for all the specified generic soil cases. The floor response spectra and broadened envelope at the center of the containment for the five soil cases analyzed in SASSI are shown in the left side of Figure 2.6-2(e). The envelopes of the broadened spectra at 7 locations of the basemat are shown in the right hand side of the figure. The spectra for the time history developed enveloping these broadened spectra are shown in Figure 2.6-2(f).

Table 2.6-2(b) compares the sum of the soil reactions on the basemat for the equivalent static accelerations applied in the design analyses of the basemat on soil springs to those obtained from linear time history analyses of the nuclear island shell model (NI20). The basemat reactions for the equivalent static analyses compare well against those of the "all soils" time history with the exception of small exceedances in the horizontal FY and vertical FZ components. The exceedance of the horizontal component is not important to the design of the basemat which is controlled primarily by vertical soil pressures induced by the vertical FZ component and the overturning moments. The exceedance of the vertical component was evaluated by comparing the bearing pressures at the corners and west edge of the nuclear island due to the vertical FZ component and the overturning moments. These bearing pressures were calculated from the basemat reactions assuming a rigid basemat for dead live and seismic loads. Seismic loads were considered using the 1.0, 0.4, 0.4 combination method. Maximum bearing pressures for the two cases are shown in Table 2.6-2(c). The bearing pressures resulting from the equivalent static accelerations are similar to those due to the "all soils" time history analysis demonstrating the adequacy of the equivalent static accelerations applied in the basemat analyses.

2.6.1.3 Normal load bearing reactions

The bearing reactions under dead and live load from the 3D ANSYS analyses on soil springs with subgrade modulus of 520 kcf are shown in Figure 2.6-3.

2.6.1.4 Normal plus seismic reactions

Liftoff analyses were performed for 16 load cases of dead, live and seismic loads for the soil site with subgrade modulus of 520 kcf. Seismic loads are applied with unit factor in one direction and with 0.4 factor in the other two directions. The 16 cases were those having the unit factor applied in the horizontal direction in order to maximize the overturning. Cases with unit factor in the vertical direction were also analyzed in linear analyses and do not control. Maximum bearing reactions at the corners of the auxiliary building and at the west side of the shield building are shown in Table 2.6-3. Bearing pressure contours are shown in Figures 2.6-4 to 2.6-8 for the five load cases resulting in these maximum bearing reactions. The seismic load combination is shown for each figure. Note that the bearing pressures reduce rapidly away from the corners. These figures show lift off for equivalent static loads which are higher than the maximum time history loads as discussed in section 2.4.2. This is particularly the case for load combinations with unit seismic load in the Y direction (East-West) where the footprint dimension is smaller. The results of the equivalent static analyses are used for basemat design. The maximum bearing capacity reactions for defining minimum dynamic soil bearing capacity are based on time history analyses as discussed in Section 2.4.2.

2.6.2 Basemat reinforcement design

The Nuclear Island basemat is a reinforced concrete structure designed in accordance with the following American Concrete Institute (ACI) standard:

ACI 349-01, Code Requirements for Nuclear Safety Related Concrete Structures

Additional reinforcement is provided in the design of the 6' mat for soil sites such that the basemat can resist loads 20 percent greater than the demand calculated by the equivalent static acceleration analyses on uniform soil springs. This increase is based on the AP600 precedent and accommodates lateral variability of the soil investigated separately in a series of parametric studies.

The reinforcement required is calculated for the member forces for each of the following load combinations.

1 1.4 x (D) + 1.7 x (H) + 1.7 x (L)

3 D + L + H +Es

9 1.4 x (D) + 1.7 x (H) + 1.7 x (L) + 1.5 x (Pd)

10 D + L + H + Pd + Es

The reinforcement is calculated for each shell element in the 6' basemat and for a series of paths through the solid elements of the DISH. Tables 2.6-4 to 2.6-8 show the reinforcement required in both the 6' basemat and the DISH. The tables also show the reinforcement provided. Reinforcement for the 6' thick mat and the DISH is provided in up to 10 layers with layer number 1 being the lowest layer at the bottom of the mat. Layers 1 and 2 are at the bottom of the 6' mat and the DISH. Layer 3 is an additional circumferential layer below the DISH. Layers 4 and 5 are at the top of the 6' mat and below the center portion of the containment vessel. Layers 6 through 10 are below the containment vessel. These layers are shown in Figures 2.6-9 and 10. The reinforcement arrangement for each layer is shown in Figure 2.6-9 to 2.6-15.

2.6.2.1 Comparison of the AP1000 to AP600 in the Two Critical Bays

The reinforcement provided for the AP1000 has been compared to the reinforcement provided for the AP600. In general the reinforcement for the AP1000 has stayed the same or has increased due to the higher bearing demand caused by the increase in height of the shield building. In a few cases the reinforcement has decreased. These cases were reviewed.

The reinforcement provided for the AP1000 between column lines 9.1 and 11 and column lines K and L is equal to or greater than that for the AP600 with the exception of the east west bottom and shear reinforcement The spacing of this reinforcement was increased from 10" to 12". This change in spacing was made to improve constructability since the dowel bars for the walls are also at multiples of 12" spacing. Review of the calculations showed that the required reinforcement in the east west direction could be reduced due to the large conservatism of the hand calculations used for the AP600 design. These hand calculations applied maximum bearing pressures at the edge of the bay to a continuous one way beam representing the middle of the bay. The AP1000 design uses directly the member forces from the finite element analysis, which considers the two way action, and permits redistribution of bearing pressures due to flexibility of the slab.

The reinforcement provided for the AP1000 between column lines 1 and 2 and column lines K-2 and N is equal to or greater than that for the AP600 with the exception of the shear reinforcement. This reinforcement was decreased from #11 to #9 to improve constructability. The required shear reinforcement decreased due to the change in assumption of one way action to the use of the member forces from the finite element analysis, which considers two way action. The use of two way action required an increase in the east west top reinforcement in this bay.

Table 2.6-1

Subgrade modulus for AP1000 Soil Cases

Soil case	Subgrade modulus
	kcf
Hard rock	6267
Firm rock	2833
Soft rock	1661
Upper bound soft to medium (water table to grade)	1509
Upper bound soft to medium (dry)	1508
Soft to medium (water table to grade)	867
Soft to medium (dry)	670
Soft soil (water table to grade)	276
Soft soil (dry)	170

Table 2.6-2(a)

Equivalent Seismic Static Accelerations for Nuclear Island Basemat Analyses

	Elevation feet	Equivalent Static Seismic Accelerations (1) X	Y	Z		Elevation feet	Equivalent Static Seismic Accelerations (1) X	Y	Z
Shield Bldg	66.5	0.3	0.3	0.3	SCV	100	0.32	0.33	0.31
& Aux Bldg	81.5	0.32	0.33	0.32		104.13	0.32	0.35	0.32
	99	0.32	0.34	0.35		112.5	0.34	0.39	0.35
	116.5	0.46	0.4	0.37		131.68	0.37	0.49	0.41
	134.88	0.6	0.47	0.38		141.5	0.42	0.54	0.44
	153.98	0.63	0.5	0.44		162	0.51	0.65	0.49
	162	0.65	0.52	0.46		169.93	0.55	0.69	0.51
	180	0.68	0.55	0.51		200	0.72	0.83	0.58
	200	0.68	0.61	0.56		224	0.89	0.97	0.63
	222.75	0.67	0.68	0.62		244.21	1.02	1.1	0.66
	242.5	0.73	0.76	0.65		255.02	1.09	1.16	0.71
	265	0.79	0.85	0.69		265.83	1.16	1.23	0.82
	294.93	0.96	1.06	0.88		273.83	1.2	1.28	0.98
	333.13	1.23	1.35	0.89		281.9	1.25	1.32	1.21
Platform	290.5	2.16	1.93	1.01	Polar Crane	233.5	1.45	2.51	1.34
CIS	60.5	0.3	0.3	0.3	CIS	107.2	0.35	0.34	0.32
	66.5	0.3	0.3	0.3		134.3	0.5	0.5	0.37
	82.5	0.31	0.31	0.3	SGE	153	0.61	0.69	0.4
	98	0.32	0.33	0.31	SGW	153	0.61	0.69	0.4
	103	0.34	0.34	0.31	Press	169	0.81	1.18	0.46

Notes:

(1) X = North-South; Y = East-West; Z = Vertical
(2) Linear interpolation between elevations is acceptable

Table 2.6-2(b)

Nuclear Island Base Reactions

Units: 1000 kips & 1000 ft-kip

Seismic Reactions		Base Reactions	
		Equivalent Static Accelerations applied to NI in Basemat Design Analyses	**Fixed Base Time History Analysis (NI20 All soils)**
Shear NS	FX	124.48	116.45
Shear EW	FY	120.51	127.51
Vertical	FZ	110.38	129.68
Moment about NS	MXX	11,357	11,700
Moment about EW	MYY	11,520	11,200

Notes:

1. Moment summation point is at the center of the shield building at EL 60'-6" (X=1000, Y=1000, Z=60.5).
2. Equivalent static results are shown for the response from one direction, (i.e FX and MYY due to X input, FY and MXX due to Y input, and FZ due to Z input.) The increase due to combination of three directions is small.
3. See Table 2.4-2 for 2D analysis results for other soils.

Table 2.6-2(c)

Maximum soil bearing pressures (ksf) at corners from basemat reactions

Location	Equivalent static accelerations Linear Analyses	Fixed base time history all soils
West side of shield building	36.8	36.9
NW corner of auxiliary building	27.1	24.8
NE corner of auxiliary building	22.8	25.5
SE corner of auxiliary building	21.1	25.1
SW corner of auxiliary building	29.6	27.1

Table 2.6-3

Maximum soil pressure at corners from equivalent static non-linear analyses

Location	Maximum bearing pressure (ksf)	Load Case	S_{NS}	S_{EW}	S_{VT}
West side of shield building	52.8	3-13	-0.4	1.0	0.4
NW corner of auxiliary building	28.9	3-2	1.0	0.4	-0.4
NE corner of auxiliary building	29.7	3-11	0.4	-1.0	0.4
SE corner of auxiliary building	26.7	3-15	-0.4	-1.0	0.4
SW corner of auxiliary building	33.1	3-5	-1.0	0.4	0.4

Table 2.6-4

Longitudinal Reinforcement, Top face of DISH in Radial and Hoop Directions (Layers 6 to 10)

<table>
<tr><th colspan="3">Zone</th><th rowspan="2">Required
(in^2/ft)</th><th rowspan="2">Provided
(in^2/ft)</th><th rowspan="2">Rebar Placement</th></tr>
<tr><th>Layer</th><th>Radius range</th><th>Direction</th></tr>
<tr><td>4</td><td>0 – 30’</td><td>NS</td><td rowspan="2">2.615</td><td>3.12</td><td>#11@6”</td></tr>
<tr><td>5</td><td>0 – 30’</td><td>EW</td><td>3.12</td><td>#11@6”</td></tr>
<tr><td>10a</td><td>17’ – 23’</td><td rowspan="6">radial</td><td>Note 2</td><td>Note 2</td><td rowspan="6">Layer 8a: #11@1.5°
Layer 8b: #11@1.5°
Layer 8c: #11@0.75°
Layer 10a: #11@1.5°
Layer 10b: #11@1.5°
Layer 10c: #11@0.75°</td></tr>
<tr><td>10a+10b</td><td>23’ – 35’(W)
23’ – 33’(E)</td><td>Note 2</td><td>Note 2</td></tr>
<tr><td>10a+10b+
8a</td><td>35’ – 42’(W)
33’ – 37’(E)</td><td>Note 2</td><td>Note 2</td></tr>
<tr><td>10a+10b+
8a+8b</td><td>42’ – 46’(W)
37’ – 49’(E)</td><td>Note 2</td><td>Note 2</td></tr>
<tr><td>10a+10b+
10c+8a+8b</td><td>46’ – 60’(W)
49’ – 53’(E)</td><td>Note 2</td><td>Note 2</td></tr>
<tr><td>10a+10b+
10c</td><td>60’–out1(W)
53’– out1(E)</td><td>Note 2</td><td>Note 2</td></tr>
<tr><td>9</td><td>30’ – 33’</td><td rowspan="5">hoop</td><td>2.96</td><td>3.12</td><td rowspan="5">Layer 7a: #11@12”
Layer 7b: #11@6”
Layer 9: #11@6”</td></tr>
<tr><td>9+7a</td><td>33’ – 40’</td><td>3.46</td><td>4.68</td></tr>
<tr><td>9+7b</td><td>40’ – 58’</td><td>5.95</td><td>6.24</td></tr>
<tr><td>9+7a (W)
9 (E)</td><td>58’ – 62’</td><td>3.01 (W)
2.2 (E)</td><td>4.68</td></tr>
<tr><td>9</td><td>62’–out1</td><td>2.37</td><td>3.12</td></tr>
</table>

Note 1: See Figure 2.6-9 and 2.6-10 for plan and elevation schematic views of the reinforcement layout.

Note 2: Figure 6-1 and 6-2 in APP-1010-CCC-004, Rev.0 provide graphical presentation of the "Required" (red dash line) and "Provided" (solid black line) areas of radial reinforcement for the top face of the Dish.

Table 2.6-5

Longitudinal Reinforcement, Top Face in NS direction (Layer 4)

Zone		Required (in^2/ft)	Provided (in^2/ft)	Rebar Placement
NS Wall Lines	**EW** Wall Lines			
General Area		Less than 2.25	2.25	#14@12"
Within Wall 1 to Wall 2	Within Wall J-2 to Wall N	2.719	3.25	#14@12" + #9@12" in one layer
East side of DISH, rectangular zone		2.418		
The four Pit Areas		0.911	1.56	#11@12"

Note: See Figure 2.6-11

Table 2.6-6

Longitudinal Reinforcement Top Face in EW direction (Layer 5)

Zone		Required (in^2/ft)	Provide d (in^2/ft)	Rebar Placement
NS Wall Lines	**EW** Wall Lines			
General Area		Less than 2.25	2.25	#14@12"
Within Wall 4 to Wall 7.3	Within Wall I to Wall J	2.758	3.25	#14@12" + #9@12" in one layer
North side of DISH		2.684		
The four Pit Areas		0.911	1.56	#11@12"

Note: See Figure 2.6-12

Table 2.6-7

Longitudinal Reinforcement, Bottom Face in NS and EW direction (Layers 1, 2 and 3)

Zone	Direction	Required (in^2/ft)	Provided (in^2/ft)	Rebar Placement
All below SB	NS (layer 1)	4.41	4.5	#14@6”
	EW (layer 2)			
West-half of DISH, radius = 50’ and more (See figure 2.6-13)	Circumference (layer 3)	4.67	1.56 Additional	#11@12” additional
All below AB	NS (layer 1)	Less than 2.25	2.25	#14@12”
	EW (layer 2)			
South side of DISH	NS (layer 1)	3.581	4.5	#14@6”
	EW (layer 2)	3.581		
North side of DISH	NS (layer 1)	3.119		
	EW (layer 2)	3.119		
East side of DISH, beneath Wall 7.3	EW	3.187	3.25	#14@12” + #9@12”
The four Pit Areas	NS (layer 1)	Less than 2.25	2.25	Same as the General Area
	EW (layer 2)			

Note: See Figure 2.6-13 and 14

Table 2.6-8

Shear Reinforcement

Zone		Required (in^2/ft^2)	Provided (in^2/ft^2)	Rebar Placement
NS Wall Lines	**EW** Wall Lines			Intervals are shown as NS x EW direction
All other below AB than listed below		Less than 0.25	0.25	#9@24” x 24”
Wall 1 to Wall 2	Between Wall J-2 to Wall N	0.469	0.50	#9@12” x 24”
Between Wall 2 to Wall 4	Wall I to Wall J-1	0.163		
Between Wall 4 to Wall 7.3	Wall I to SB	0.382		
SB to Wall 10	Between Wall K to Wall P	0.328		
EL62’-0” pit to near Wall I, south side*		0.764	1.24	#5@6 x 6”
EL62’-0” pit to near Wall I, north side*		0.962		
EL63’-6” pit to South near Wall I		0.739		
EL62’-0” Pit to South side of DISH		0.181	0.62	#5@6 x 12”

Note: See Figure 2.6-15

Table 2.6-9

Comparison of the AP1000 to AP600 in the Two Critical Bays

Applicable Column Lines	Elevation Level Range	Concrete Thickness	Reinforcement Type		Rebar Arrangement	Reinforcement Provided
Column line K to L and from Col. Line 11 wall to the intersection with the shield building	From EL 60' 6" to 66' 6"	6'-0"	Top Reinforcement	AP1000	NS: #14@12" EW: #14@12"	NS: $2.25in^2/ft$ EW: $2.25in^2/ft$
				AP600	*NS: #11@12"* *EW: #14@10"*	*NS:* $1.56in^2/ft$ *EW:* $2.7in^2/ft$
			Bottom Reinforcement	AP1000	NS: #14@12" EW: #14@12"	NS: $2.25in^2/ft$ EW: $2.25in^2/ft$
				AP600	*NS: #14@12"* *EW: #14@10"*	*NS:* $2.25in^2/ft$ *EW:* $2.7in^2/ft$
			Shear Reinforcement	AP1000	#9@24"(NS) x @24"(EW)	$0.25in^2/ft^2$
				AP600	*#9 @20"(NS) x @24"(EW)*	$0.3in^2/ft^2$
Column line 1 to 2 and from Column Line K-2 to N wall	From EL 60' 6" to 66' 6"	6'-0"	Top Reinforcement	AP1000	NS: #14@12", and Locally #14@12"+#9@12" EW: #14@12"	NS: $2.25in^2/ft$ Locally 3.25^2/ft EW: $2.25in^2/ft$
				AP600	*NS: #11@12" (#11@6" for 17'-0" from Wall_1)* *EW: #11@12"*	*NS:* $1.56in^2/ft$ *(*$3.12in^2/ft$ *for 17'-0" from Wall_1)* *EW:* $1.56in^2/ft$
			Bottom Reinforcement	AP1000	NS: #14@12" EW: #14@12"	NS: $2.25in^2/ft$ EW: $2.25in^2/ft$
				AP600	*NS: #14@12" (#14@6" for 7'-6" from Wall_2)* *EW: #14@12"*	*NS:* $2.25in^2/ft$ *(*$4.5in^2/ft$ *for 7'-6" from Wall_2)* *EW:* $2.25in^2/ft$
			Shear Reinforcement	AP1000	#9@12"(NS) x @24"(EW)	$0.50in^2/ft^2$
				AP600	*#11 @12"(NS) x @24"(EW)*	$0.78in^2/ft^2$

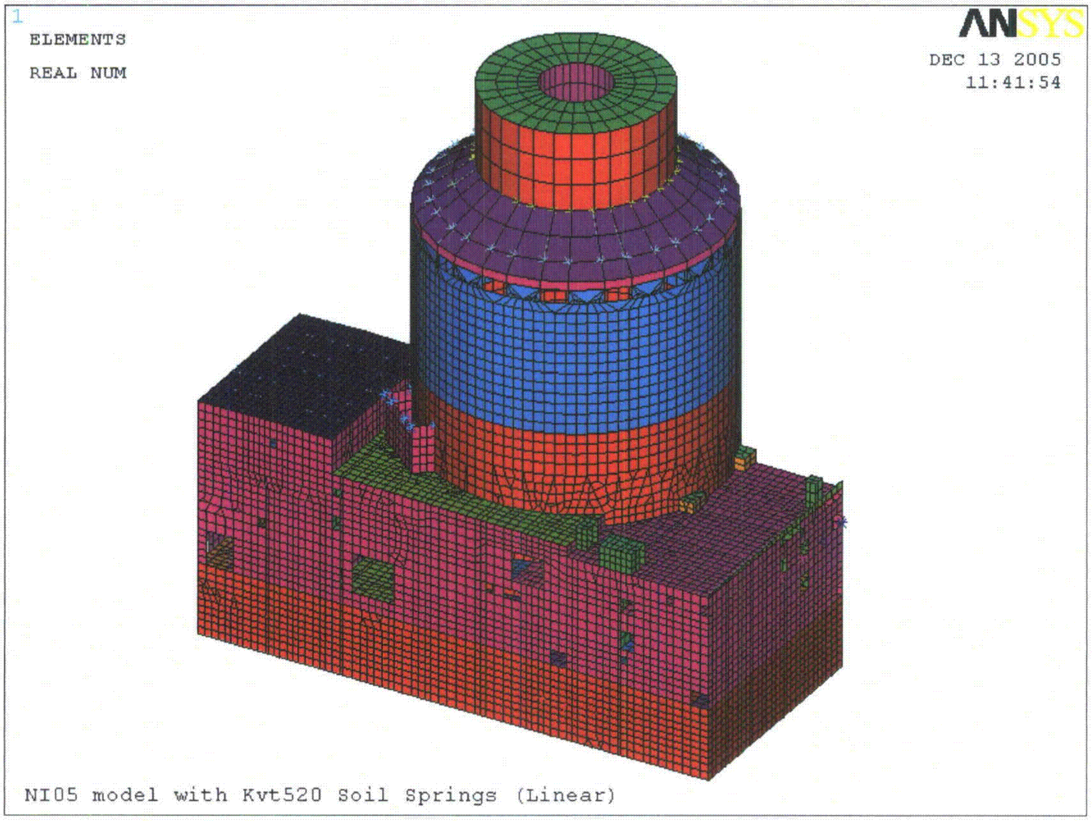

Figure 2.6-1 NI05 Model with Soil Springs

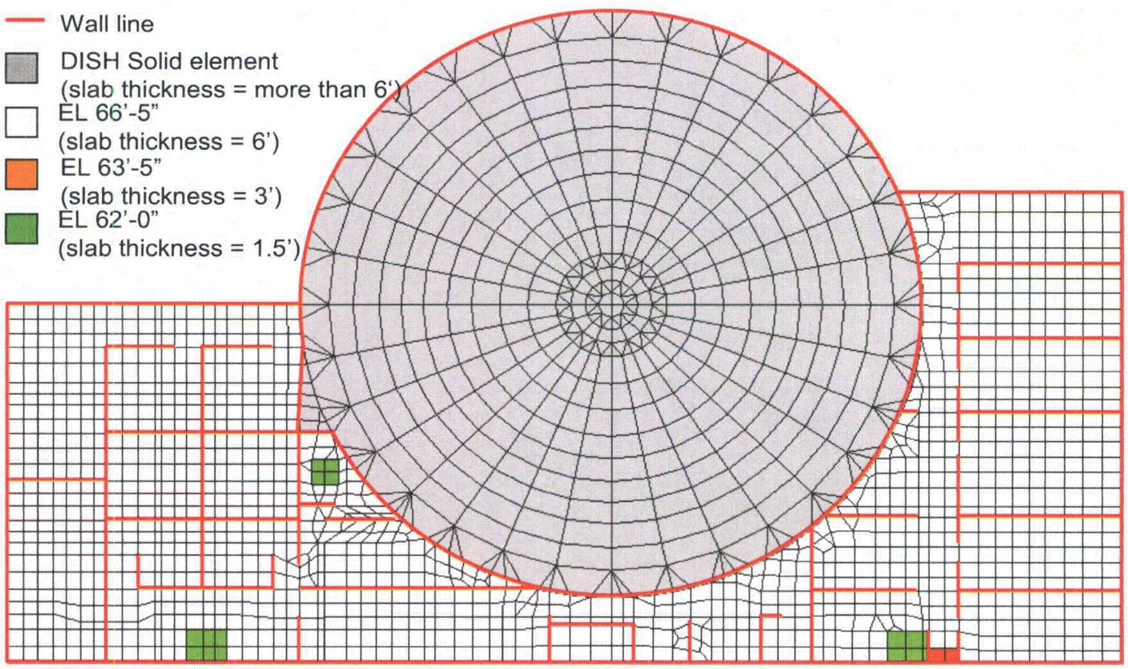

Figure 2.6-2 Basemat Elements along with Wall Lines above the Basemat

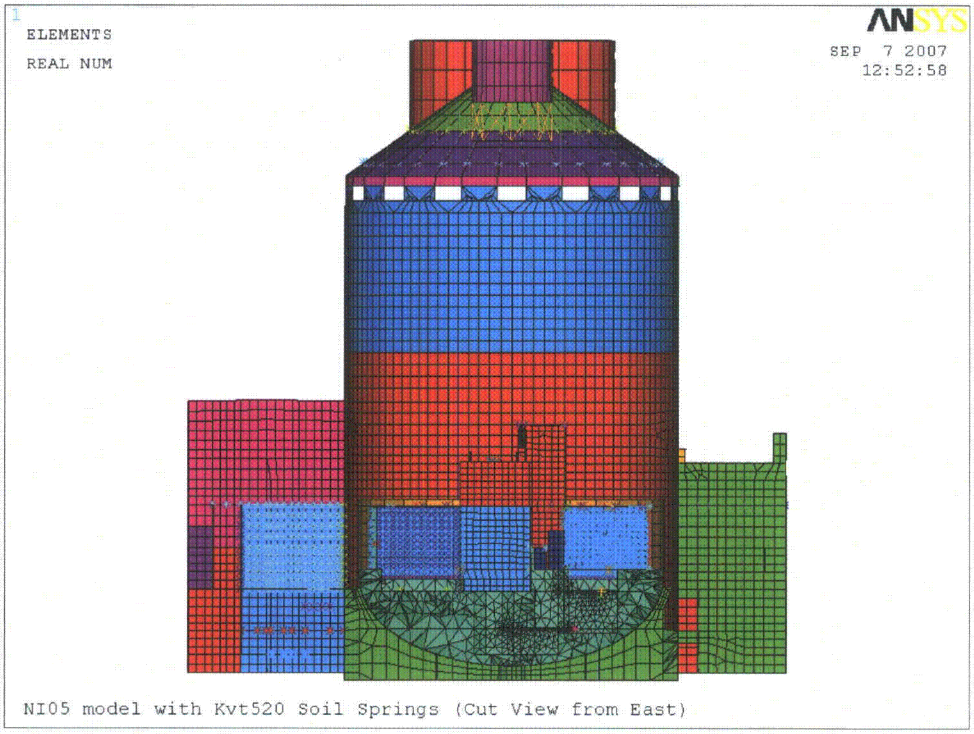

Figure 2.6-2 (a) Section View of NI05 Model from East

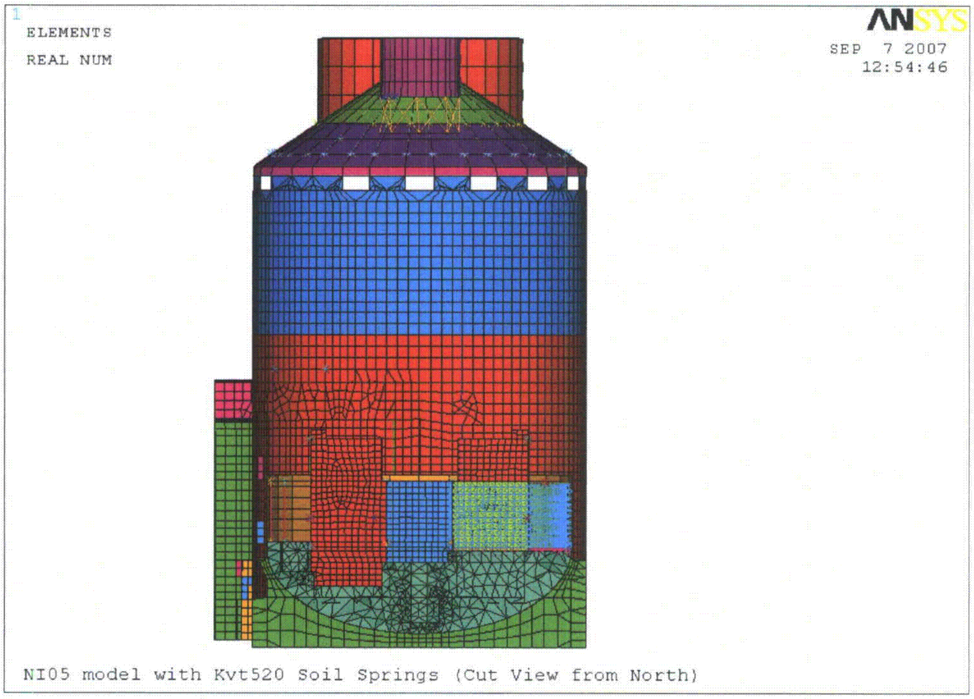

Figure 2.6-2 (b) Section View of NI05 Model from North

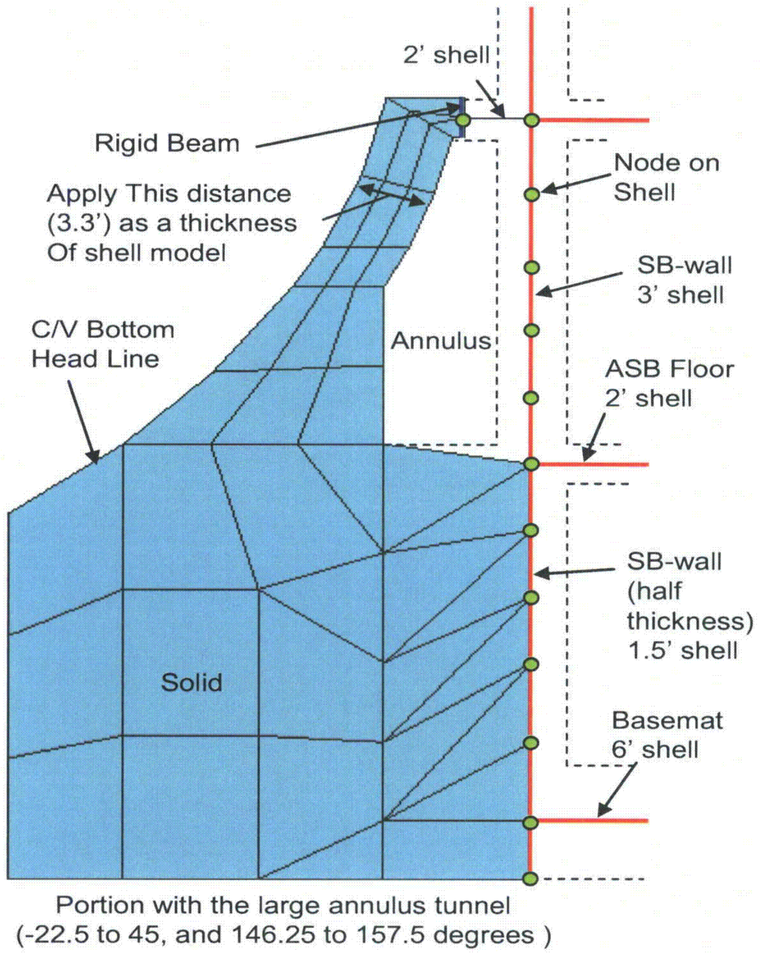

Figure 2.6-2 (c) Typical Connection of Auxiliary Building to Dish

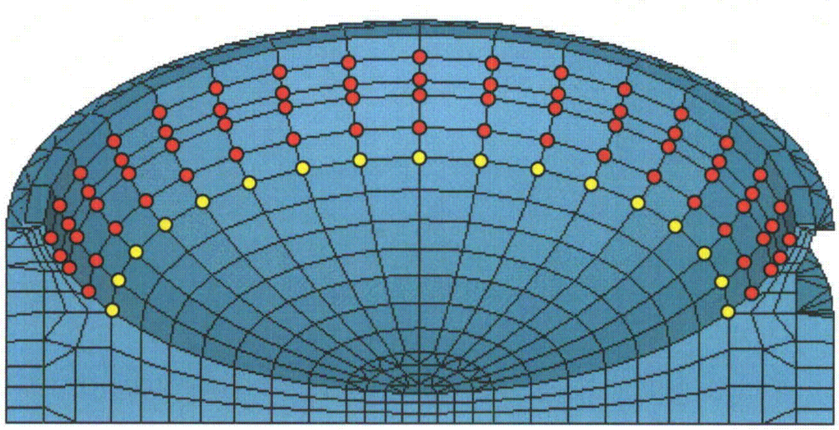

Figure 2.6-2 (d) Connection Nodes between Containment Vessel and Dish

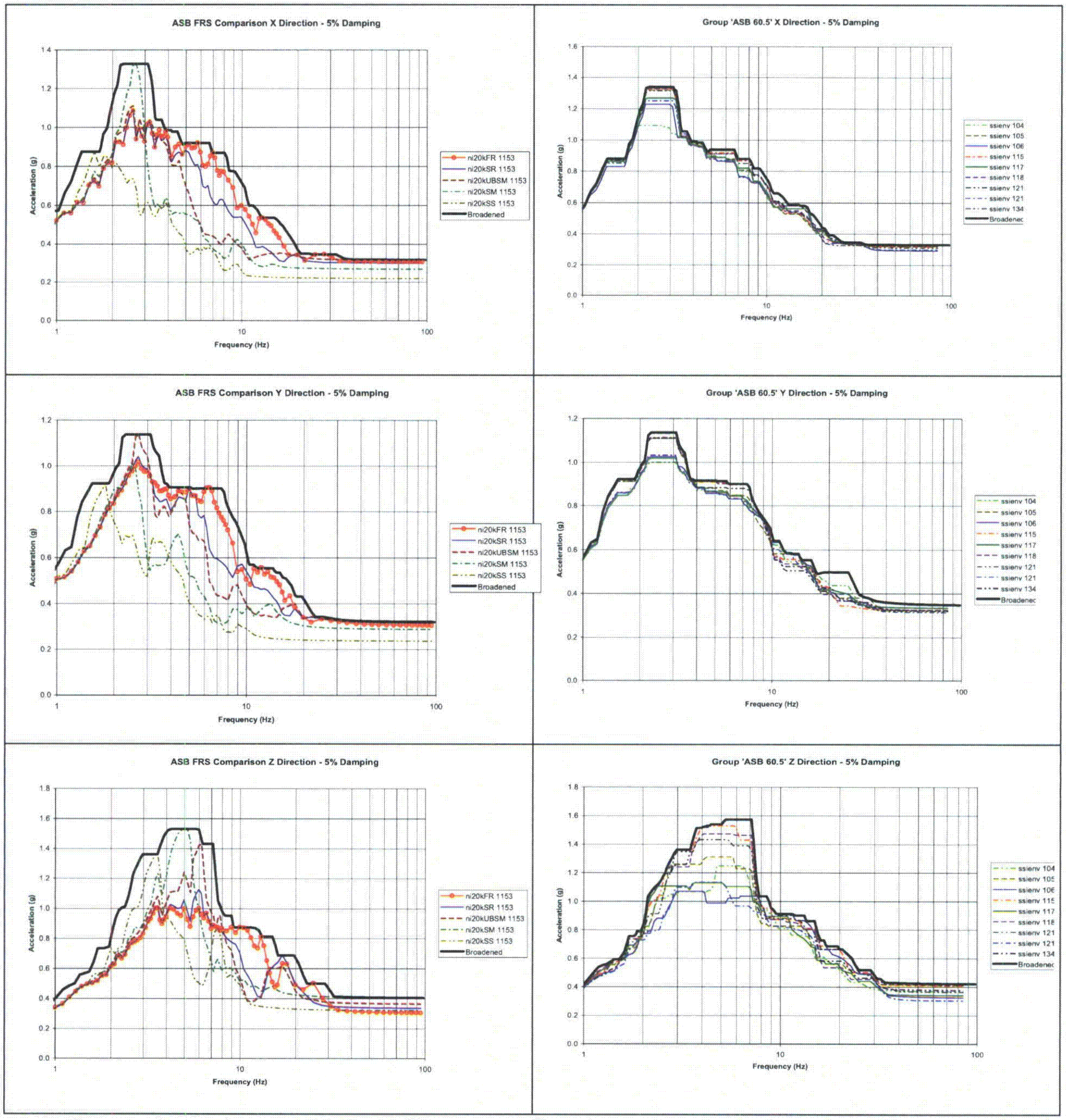

Center of containment (Node 1153) Envelope of center and corners of basemat

Figure 2.6-2(e) Basemat response spectra from SASSI analyses

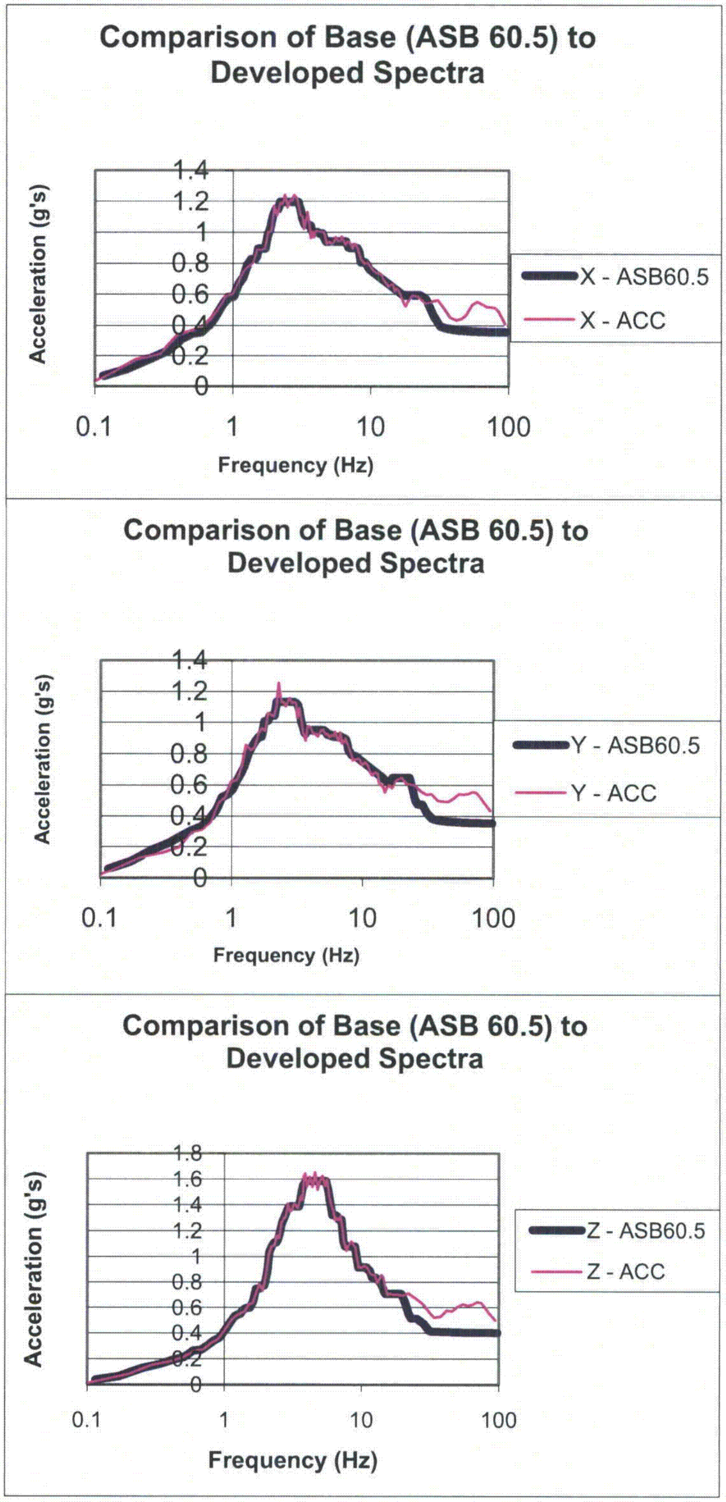

Figure 2.6-2 (f) Comparison of Time History Response Spectra against 'ASB 60.5' envelope

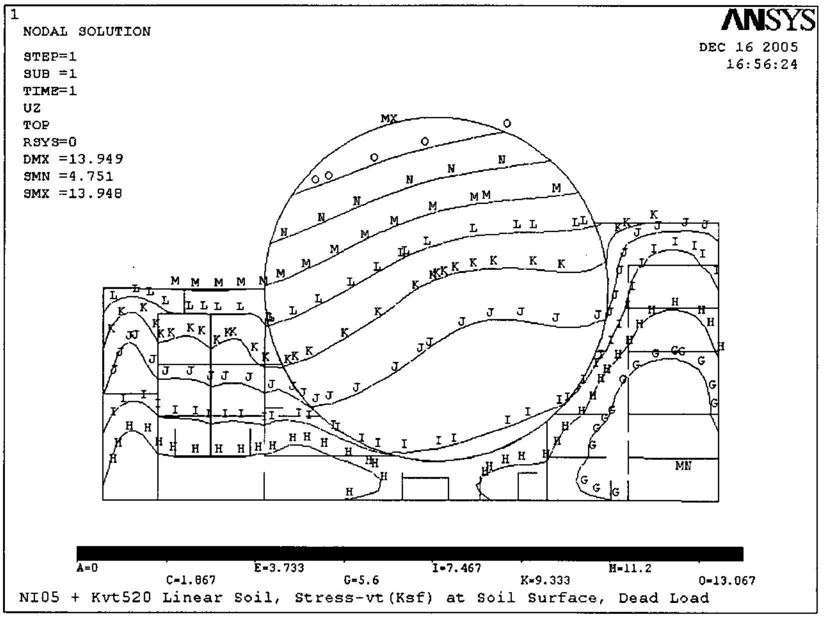

Bearing Pressure under DL, Linear Analysis

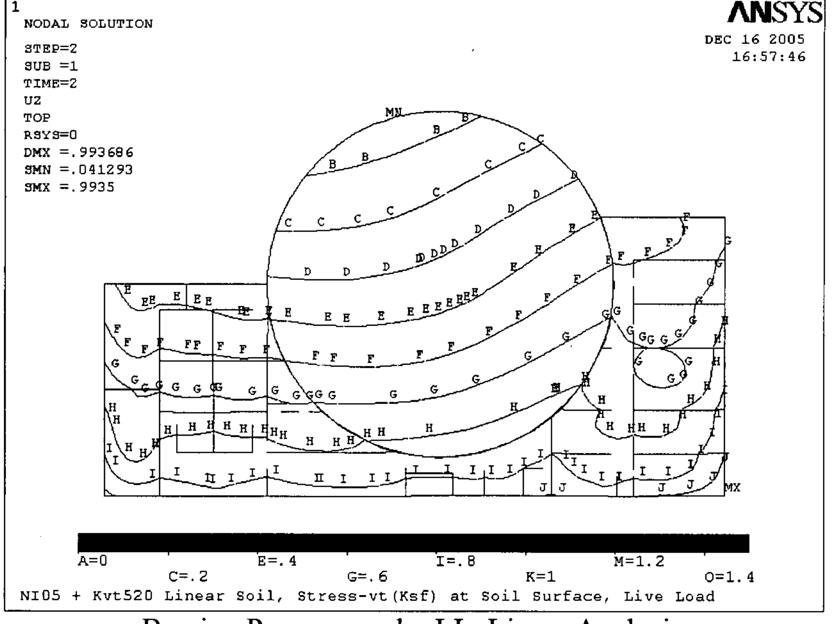

Bearing Pressure under LL, Linear Analysis

Figure 2.6-3 Soil Bearing Pressure for Normal Operating Loads

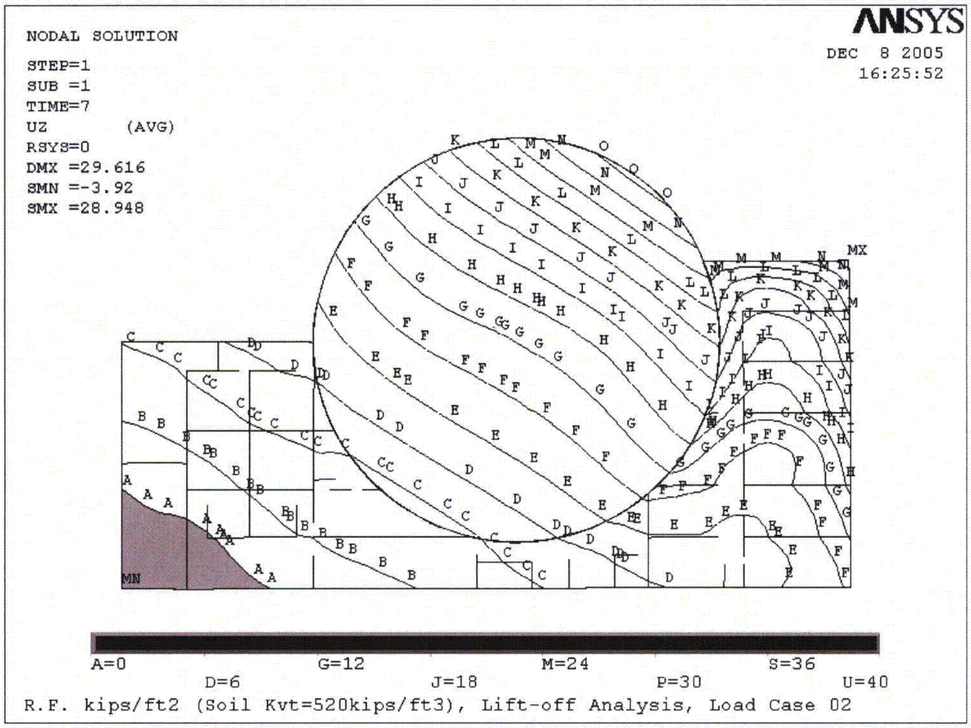

Figure 2.6-4 Soil Bearing Pressure in Load Case 3-2 (Es= 1.0xSns+0.4xSew-0.4xSvt)

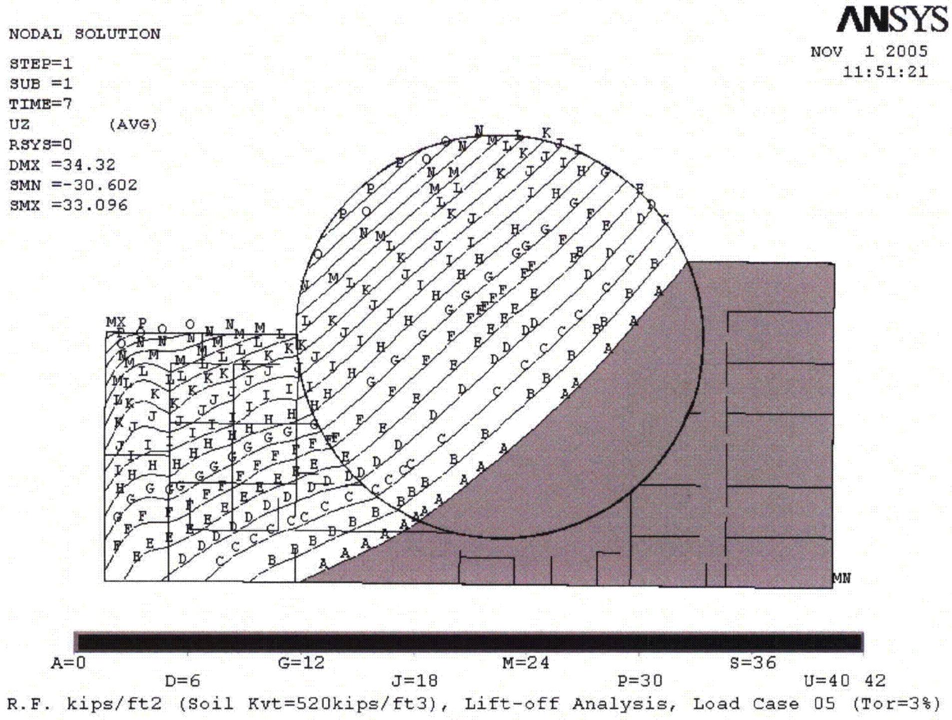

Figure 2.6-5 Soil Bearing Pressure in Load Case 3-5 (Es= -1.0xSns+0.4xSew+0.4xSvt)

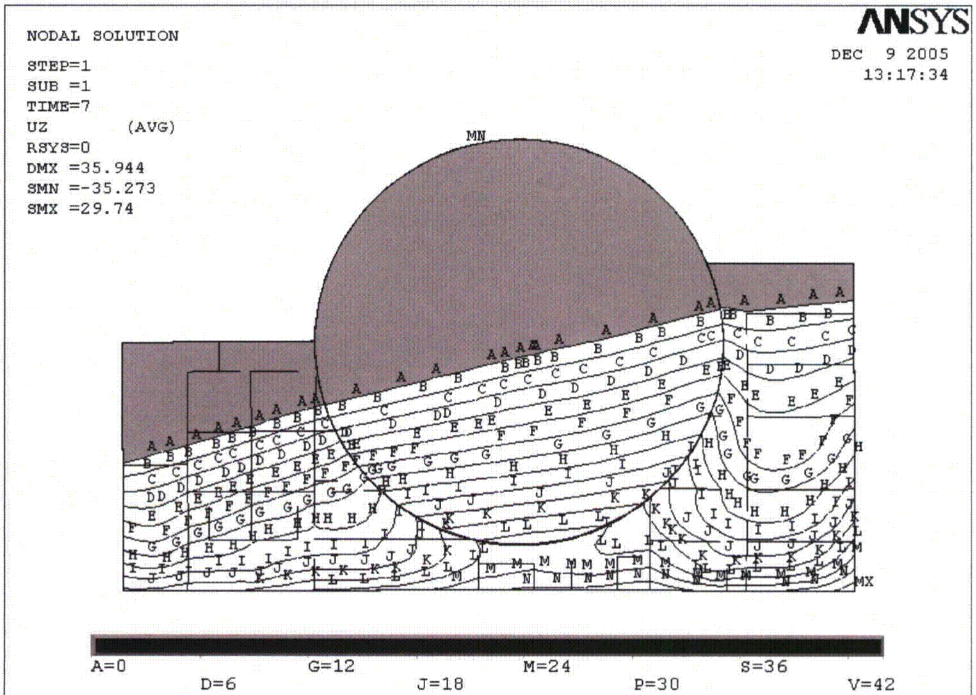

R.F. kips/ft2 (Soil Kvt=520kips/ft3), Lift-off Analysis, Load Case 11

Figure 2.6-6 Soil Bearing Pressure in Load Case 3-11 (0.4xSns-1.0xSew+0.4xSvt)

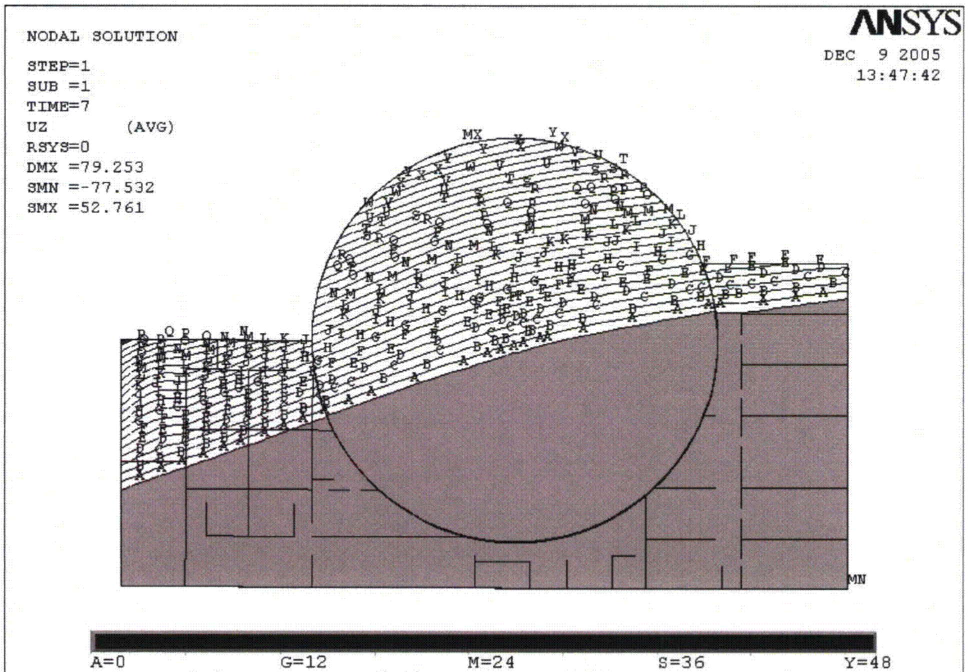

R.F. kips/ft2 (Soil Kvt=520kips/ft3), Lift-off Analysis, Load Case 13

Figure 2.6-7 Soil Bearing Pressure in Load Case 3-13 (-0.4xSns+1.0xSew+0.4xSvt)

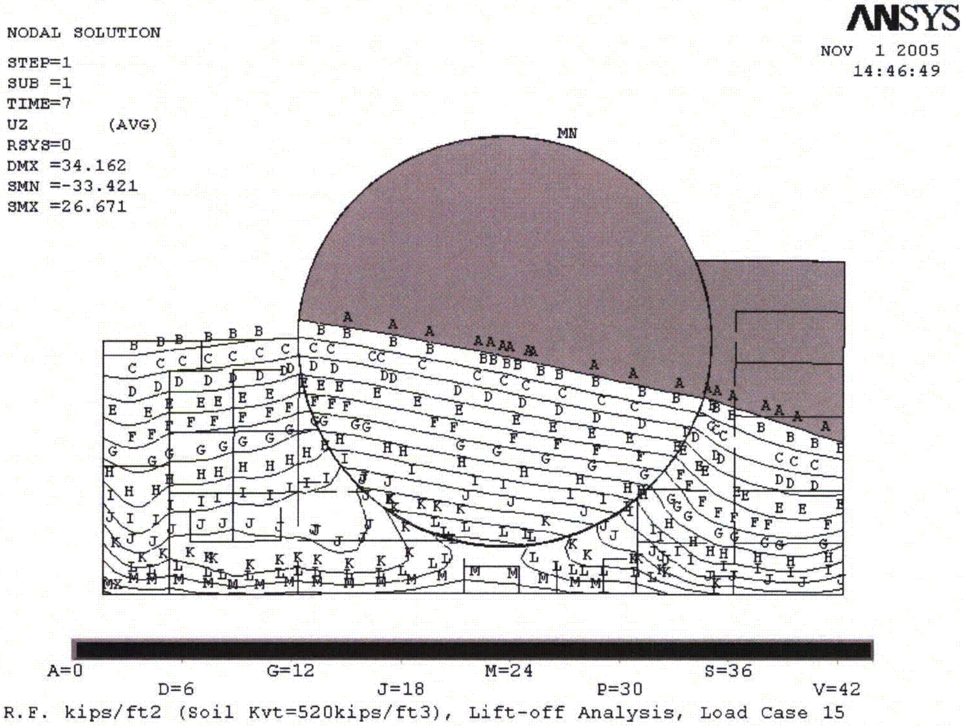

Figure 2.6-8 Soil Bearing Pressure in Load Case 3-15 (-0.4xSns-1.0xSew+0.4xSvt)

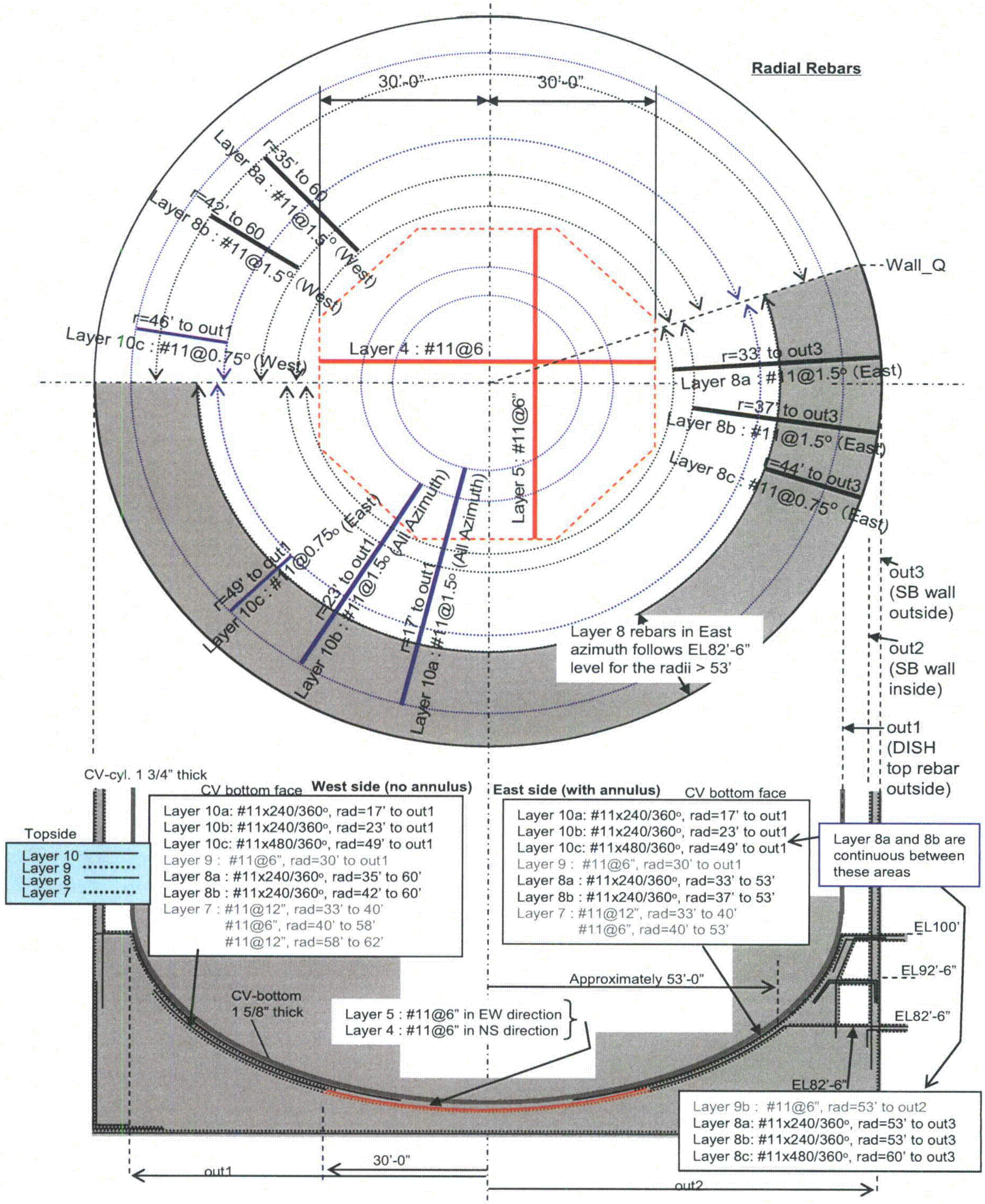

Figure 2.6-9 Radial Reinforcement, Top side of DISH

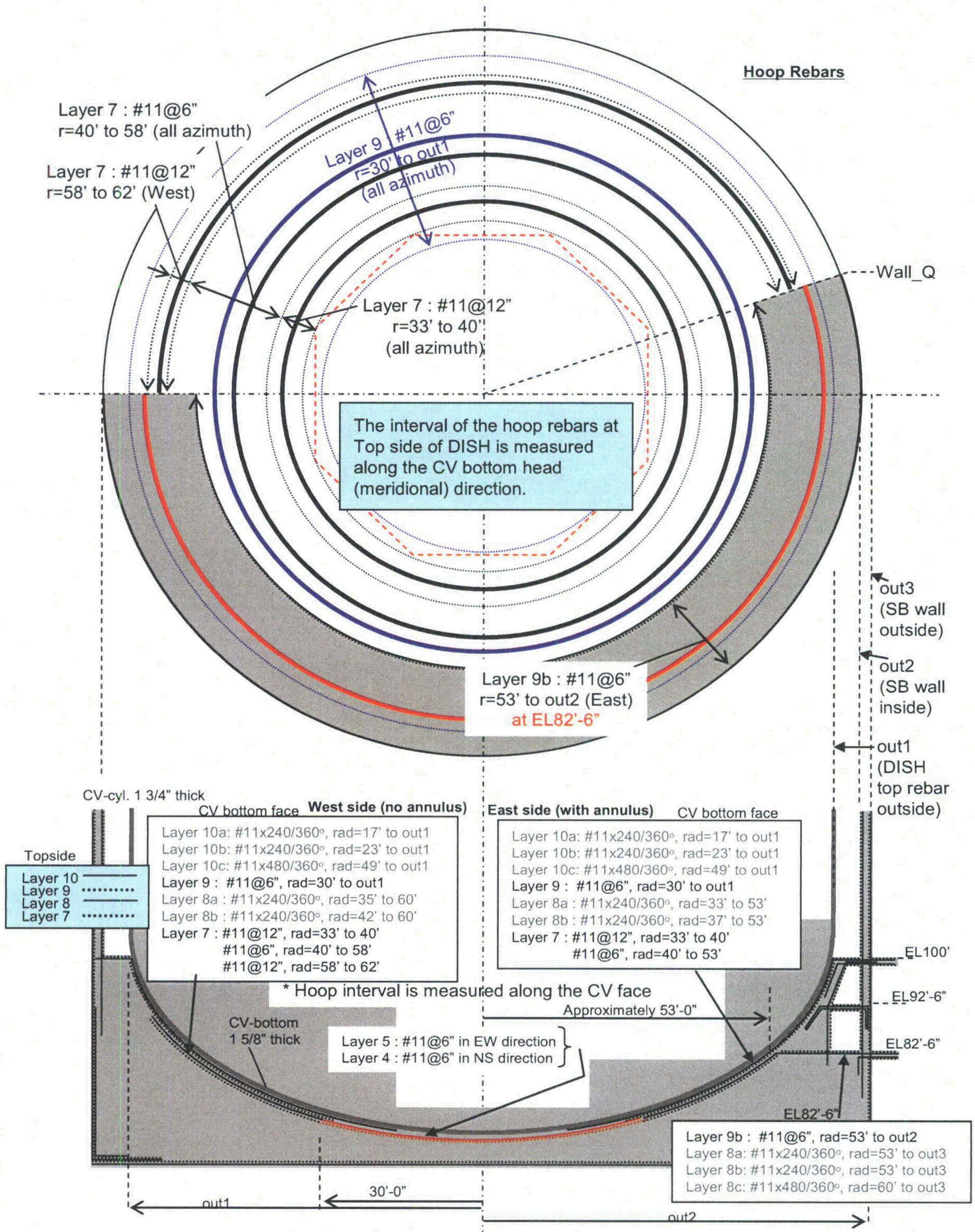

Figure 2.6-10 Circumferential Reinforcement, Top side of DISH

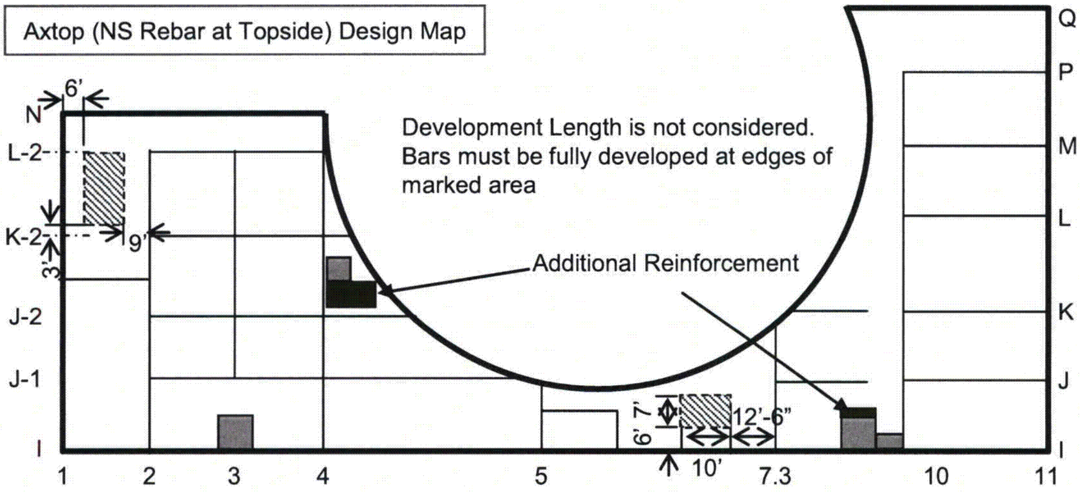

Rebar arrangement	□ : #14@12" ▨ : #14@12"+#9@12"	■ : #11@12"
Location	Layer 4	Top side of the 1.5' & 3' thick Pits

Figure 2.6-11 Longitudinal Reinforcement Map, Top side in NS direction

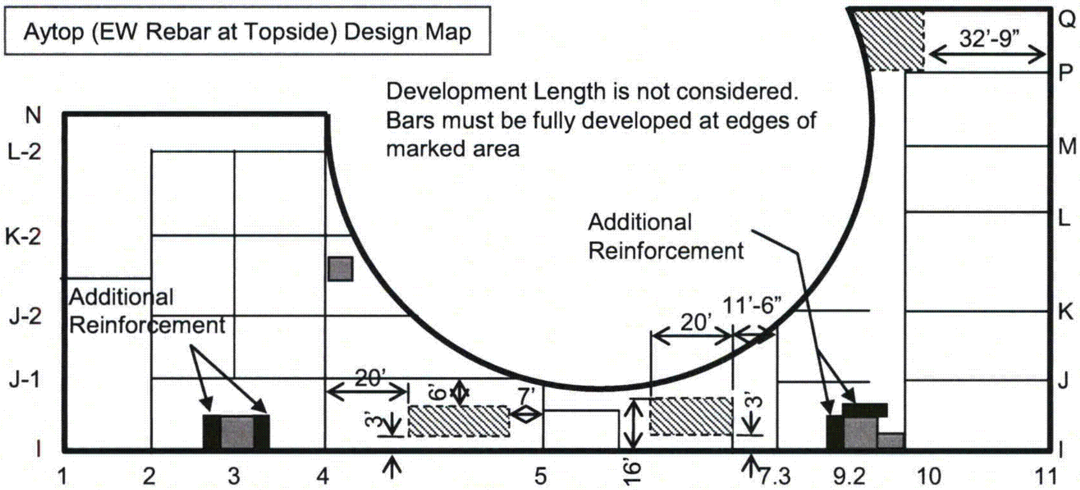

Rebar arrangement	□ : #14@12" ▨ : #14@12"+#9@12"	■ : #11@12"
Location	Layer 5	Top side of the 1.5' & 3' thick Pits

Figure 2.6-12 Longitudinal Reinforcement Map, Top side in EW direction

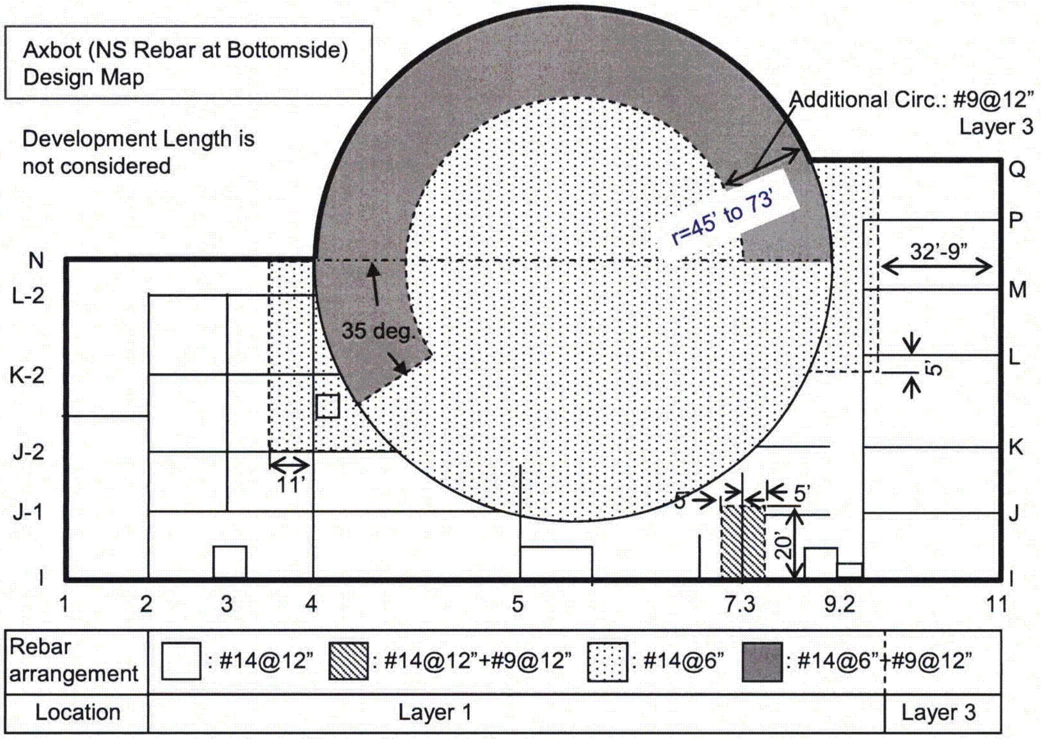

Figure 2.6-13 Longitudinal Reinforcement, Bottom side of DISH and 6' basemat (NS)

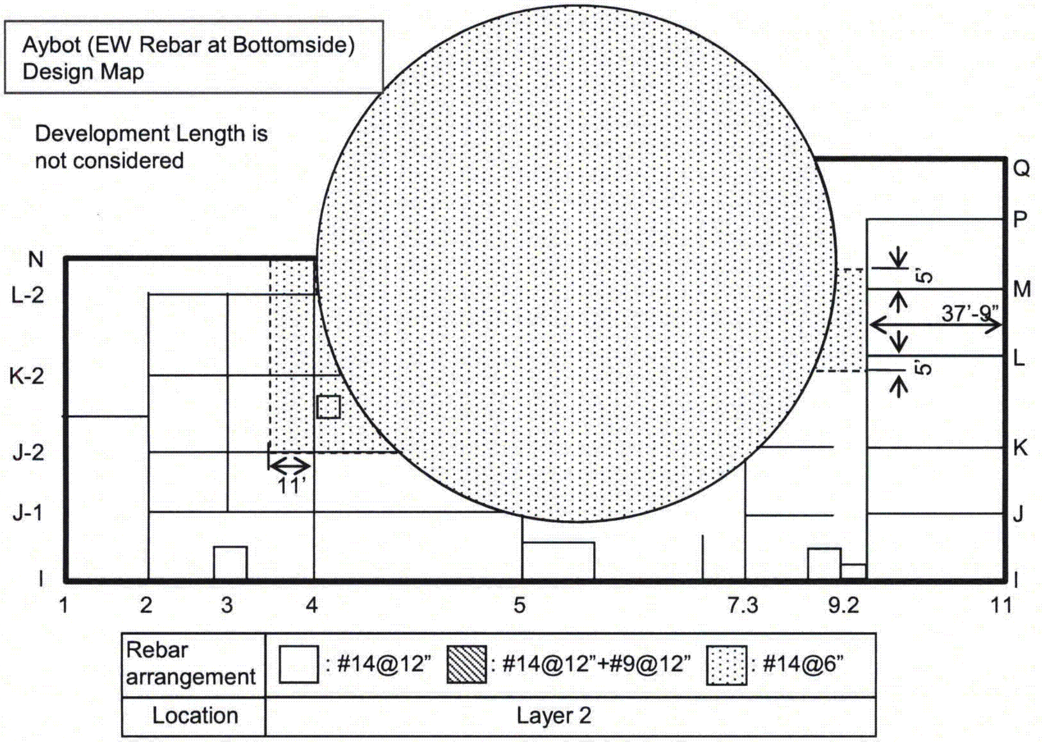

Figure 2.6-14 Longitudinal Reinforcement, Bottom side of DISH and 6' basemat (EW)

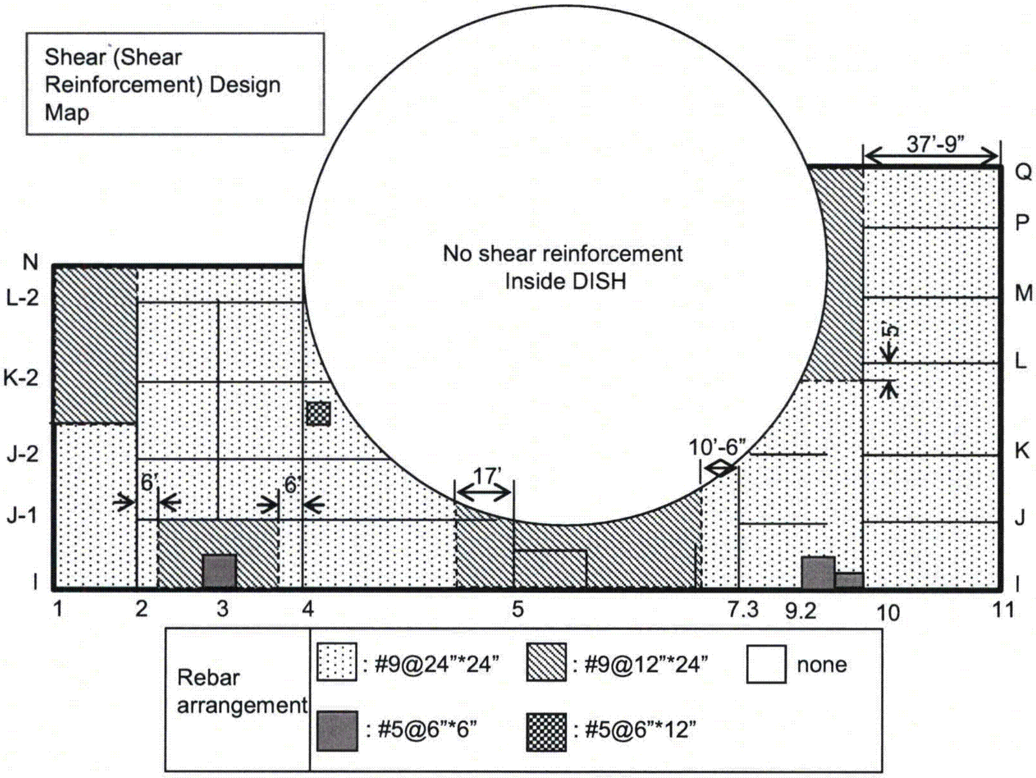

Figure 2.6-15 Shear Reinforcement Map

2.7 Basemat design studies

2.7.1 Soil modeling

2.7.1.1 Effect of Lower Stiffness Soil Springs

A study was performed to investigate the effect of a reduced subgrade modulus on the reinforcement required in the 6' basemat of the AP1000 Nuclear Island on soil sites. The study used the nuclear island finite element model on soil springs with subgrade moduli of 520 and 260 kcf. Lift-off analyses similar to the design analyses were performed on selected critical cases. Reinforcement required for the basemat was calculated for each case. This study concluded that the reinforcement design for the basic design case using a subgrade modulus of 520 kcf with the margin of 20% used in design would envelope the results with the subgrade modulus of 260 kcf.

A subgrade modulus of 260 kcf corresponds to the soft site in the SASSI analyses where the overturning moment is only 53% of the soft to medium soil overturning. This case does not need to be considered further.

2.7.1.2 Comparison of soil finite element ANSYS models versus subgrade springs

A study was performed to investigate the effect of soil modeling. Finite element models of soil were combined with a fine mesh Nuclear Island model (NI10) with a simple CIS portion as shown in Figure 2.7-1. Most cases were performed for dead load only. One case was analyzed for horizontal loads. The cases are summarized in Table 2.7-1. Deflections, soil stresses and member forces in the basemat were compared against those obtained using Winkler springs.

2.7.1.2.1 Effect of soil depth under vertical loads

The first parametric study with these models was performed for dead loads to investigate soil bearing characteristics and basemat member forces for a soil site represented by the subgrade modulus of 520kcf. As the subgrade modulus only defines a vertical stiffness (Kvt) at the soil surface, soil models can take several patterns (soil layer depth with appropriate soil stiffness) of soil structures. In these models, embedment of NI building is not considered.

In Table 2.7-1 Model-W has Winkler springs with subgrade modulus of 520 kcf. Soil model H has soil to a depth of 816' below the foundation of the nuclear island. Soil models named L"nnn" have a surface soil depth of "nnn" feet. The elastic modulus of the soil elements, as shown in the table, is adjusted to have the same vertical stiffness as the Winkler spring of 520 kcf.

Figure 2.7-2 shows a typical comparison of the bearing pressure under dead load. Section (a) is along an east west section through the south end of the auxiliary building. Section (c) is along an east west section through the north end of the auxiliary building.

The solid soil models show higher bearing pressures at the edges (Boussinesq distribution) than the Winkler springs. The ratio of the higher bearing pressures at the edge is influenced by the soil modeling. These higher bearing pressures at the edges reduce the bearing pressures away from the edges.

The figures show the effect of the relative stiffness of the soil versus the 6 foot thick basemat and superstructure. There is significant variation in bearing stress between a location below the walls of the auxiliary building and a location at mid span between the walls. This difference is largest for Model-H with the largest soil modulus. The soil acts to stiffen bending of the mat. The soil properties analyzed range from soft rock (Model-H) to soft soil (Model-L020).

Member forces of the 6' basemat in solid soil models are generally smaller for out-of-plane forces when compared with the Winkler spring model (see also discussion in Section 2.7.2). The solid soil cases with the thinner layers of soil below the basemat respond closer to the Winkler springs.

2.7.1.2.2 Effect of side soils under vertical loads

A second parametric study investigated the effects of embedment modeling. The soil model for this case used the soil properties for the "soft to medium" soil case (Vs = 939 fps at surface to 1675 at 120 feet, Vp = 5000 fps full height assuming water to grade). This has an equivalent subgrade modulus higher than the cases described in subsection 2.7.1.2.1. In these models, the effect of the embedment of the NI building up to the grade level is considered. Three cases of side soil connectivity were considered.

Bearing pressures are shown in Figure 2.7-3 for the same east west sections at the south and north end of the auxiliary building. The distribution is similar to that of Figure 2.7-2. The side soil effect in vertical loading tends to reduce the higher bearing forces at the edge observed in the results in Figure 2.7-2. The weight of the side soil reduces the difference in vertical stress between the area beneath the basemat and the adjacent areas.

2.7.1.2.3 Horizontal loads

A third parametric study investigated characteristics of horizontal loading. One representative finite element soil model in the first study and the conventional Winkler spring model were compared. Vertical bearing reactions at the edge under horizontal loading are similar to those for loading in the vertical direction.

2.7.1.2.4 Conclusion of study

The analyses with finite element models of the soil were performed as linear elastic analyses. They require much greater computer running time and do not lead to significantly better results. The design analyses are non-linear to consider lift off. They require a more detailed model of the nuclear island than that used in the studies. They must address more combinations of seismic input than used in the studies. Hence Winkler springs were selected for use in the design analyses similar to those used in the AP600 analyses.

As discussed in section 2.7.1.2.1, the models with finite element representation of the soils show larger bearing reactions at the edges than the Winkler spring model. These higher reactions at the edges give a corresponding reduction of bearing reactions and member forces away from the edges. Hence the uniform Winkler springs are conservative for design of the basemat since reinforcement in the basemat is controlled by member forces below the center of each panel and the interior walls (the exterior wall acts more like a simple support than a fixed support).

2.7.2 VECTOR analyses

A study was performed to assess the behavior of the basemat and its interaction with the soil. The two critical bays of the basemat in the north and south west corners were modeled as single or multi-span deep beams using the University of Toronto VECTOR2 F/E software. This software is primarily a development tool based on the state-of-the-art of reinforced concrete research. The theoretical bases of VecTor2 are the Modified Compression Field Theory (MCFT) (Reference 8) and the Disturbed Stress Field Model (Reference 9) – analytical models for predicting the response of reinforced concrete elements subject to in-plane normal and shear stresses. VecTor2 models cracked concrete as an orthotropic material with smeared, rotating cracks. Originally, VecTor2 employed the constitutive relationships of the MCFT. Subsequent developments have incorporated alternative constitutive models for a variety of second-order effects including compression softening, tension stiffening, tension softening, and tension splitting. Also, the capabilities of the VecTor2 have been augmented to model concrete expansion and confinement, cyclic loading and hysteretic response, construction and loading chronology for repair applications, bond slip, crack shear slip deformations, reinforcement dowel action, reinforcement buckling, and crack allocation processes.

Over a period of more than twenty years, VECTOR2 constitutive relations for reinforced concrete were corroborated, refined and validated by extensive test programs at the University of Toronto as well as at several other research establishments, involving hundreds of test specimens. The conditions investigated have encompassed a wide range of specimen construction details and loading conditions. In all cases, the MCFT was able to accurately predict behavior in terms of crack patterns, deformations, reinforcement stresses, ultimate strengths and failure modes. Detailed comparisons of experimental versus theoretical response, for each of the test series, are found in literature.

The multi span model for the bay below the north auxiliary building is shown in Figure 2.7-4. Longitudinal reinforcement is #14@12" with 2" cover, top and bottom, and transverse stirrups are #9@24"x24". The reinforcement is modelled as bilinear with an elastic modulus of 30000 ksi up to yield and 1428 ksi beyond yield. Three commonly used analytical models were considered for the soil contact stresses:

a) Uniformly Distributed Load (UDL) as shown in Figure 2.7-5.
b) Winkler springs as shown in Figure 2.7-6 with vertical stiffness of 520 kcf.
c) Half-space granular soil layer coupled with the basemat contact nodes as shown in Figure 2.7-7. Soil properties match the 520 kcf vertical stiffness used in Case (b).

The VECTOR2 program considers cracking of the concrete and non-linear behavior of the reinforcement. Structural response is calculated up to failure for a monotonically applied uniformly distributed load in case (a) and for monotonically applied vertical displacement of the shear walls for cases (b) and (c). The results of the analyses are summarized in Table 2.7-2.

The peak vertical and horizontal deformations of the basemat relative to its supports for the three soil-structure interaction models are plotted in Figure 2.7-8 as a function of the average applied load. All models are linearly elastic up to about 0.53 Mpa (11 Ksf) and have fairly equal stiffness. This initial range represents the behavior of uncracked concrete. Beyond this loading, however, the UDL and springs models exhibit significant stiffness degradation, with clearly distinguishable cracking, yield and strain hardening zones. The half-space model shows far less stiffness degradation since the longitudinal rebar remains within the elastic range due to horizontal restraint from the soil.

Contact stresses are shown along the length of the mat for the spring and half space model in Figures 2.7-9 and 2.7-10 respectively. The contact stresses are shown at various loading steps. As the loading increases and the reinforced concrete mat stiffness reduces, contact stresses redistribute from the mid span of each bay towards the supports. They also redistribute from the long span which is most flexible to the shorter adjacent spans. The contact stresses in the soil are fairly high as the concrete slab approaches failure and could result in soil failure prior to the reinforced concrete failure. The validity of the elastic soil model for sand sites was confirmed in a separate analysis in ANSYS in which the soil was modeled with Drucker-Prager non-linear properties with an internal friction coefficient of 35 degrees. This analysis with Drucker-Prager non-linear properties showed the same failure in the reinforced concrete with no failure in the cohesionless soil.

The study leads to the following conclusions:

- In terms of average contact pressures, the UDL model grossly underestimates the failure loads, being only about 56% of Winkler springs and 35% of half-space
- The higher average load capacity of the Winkler springs model is caused by load re-distribution
- The UDL and Winkler springs models exhibit significant horizontal deformations caused by concrete dilation in the post-cracking regime
- Though not exceeding the frictional capacity, significant contact shear forces develop between the basemat and the soil in the half-space model as a result of resistance to the concrete dilation
- Similar to the Boussinesq stress distribution, contact stresses below the loaded walls within 6' of the edge of the basemat in the half space model are sharply higher than elsewhere
- Contact shear stresses, due to their post-tensioning effect on the underside of the basemat, cause a reduction of the rebar stresses, partial closing of the shear cracks and a significant increase in the basemat stiffness and its failure load
- Consideration of soil structure interaction demonstrates the capacity margin built into the AP1000 reinforced concrete basemat which is designed to ACI 349 using conventional design analysis methods with Winkler springs.

Table 2.7-1
Soil models for dead load analyses

Model name	Soil Model	Soil Property	VS (fps)	Depth of Soil below found.	Embed -ment	Boundary to Side Soil
Model-W	Spring	Kvt=520kcf			None	N/A
Model-H	Solid	E=59,000ksf, ν=0.35	2529	816'		
Model-L240	Solid	E=44,500ksf, ν=0.35	2196	240'		
Model-L120	Solid	E=31,000ksf, ν=0.35	1833	120'		
Model-L080	Solid	E=23,000ksf, ν=0.35	1579	80'		
Model-L040	Solid	E=12,000ksf, ν=0.35	1141	48'		
Model-L020	Solid	E=6,100ksf, ν=0.35	813	24'		
Model-E080a	Solid	Soft to medium soil profile			40'	Free to side soil
Model-E080b	Solid	Soil Depth=120' below grade				Half-fix to side soil
Model-E080c	Solid					No side soil layers

Note: The weight of the soil was not considered in the analyses using models W, H and L.
The weight of the soil was considered in the E models.

Table 2.7-2: Summary of results for VECTOR2 North West Analyses

Case	Elastic limit	Initial strain hardening(*)						
	Average Contact Pressure	Average Contact Pressure	Max. Contact Pressure	Min. Contact Pressure	Support Displ.	Max. Vert. Def.	Max. Horiz. Def.	Max. Crack Size
NWUDL	0.53 Mpa (11 Ksf)	1.15Mpa (24 Ksf)	N/A	N/A	N/A	7.1 mm (0.28in)	3.5 mm (0.14in)	1.8 mm (0.07in)
NWSPR	0.53 Mpa (11 Ksf)	1.44Mpa (30 Ksf)	1.72Mpa (36 Ksf)	1.0 Mpa (21 Ksf)	19.0mm (0.75in)	6.9 mm (0.27in)	5.5 mm (0.22in)	2.2 mm (0.09in)
NWHALF SP	0.72 Mpa (15 Ksf)	Rebar does not reach strain hardening						

		90 % of ultimate(**)						
Case		Average Contact Pressure	Max. Contact Pressure	Min. Contact Pressure	Support Displ.	Max. Vertical Def.	Max. Horiz. Def.	Max. Crack size
NWUDL		1.34Mpa (28 Ksf)	N/A	N/A	N/A	23.0mm (0.9 in)	13.0mm (0.51in)	6.1 mm (0.24in)
NWSPR		2.4 Mpa (50 Ksf)	3.35Mpa (70 Ksf)	1.0 Mpa (21 Ksf)	35.6mm (1.4 in)	23.0mm (0.9 in)	32.0mm (1.26in)	7.2 mm (0.28in)
NWHALF SP		3.83Mpa (80 Ksf)	10.0Mpa (210Ksf)	1.44Mpa (30 Ksf)	53.3mm (2.1 in)	6.0 mm (0.24in)	2.5 mm (0.1 in)	1.7 mm (0.07in)

Note(*): For NWUDL and NWSPR only. Rebar does not reach strain hardening for NWHALFSP

Note(**): For NWUDL and NWSPR, this represents 90% of ultimate rebar stress. For NWHALFSP it represents 90 % of shear failure.

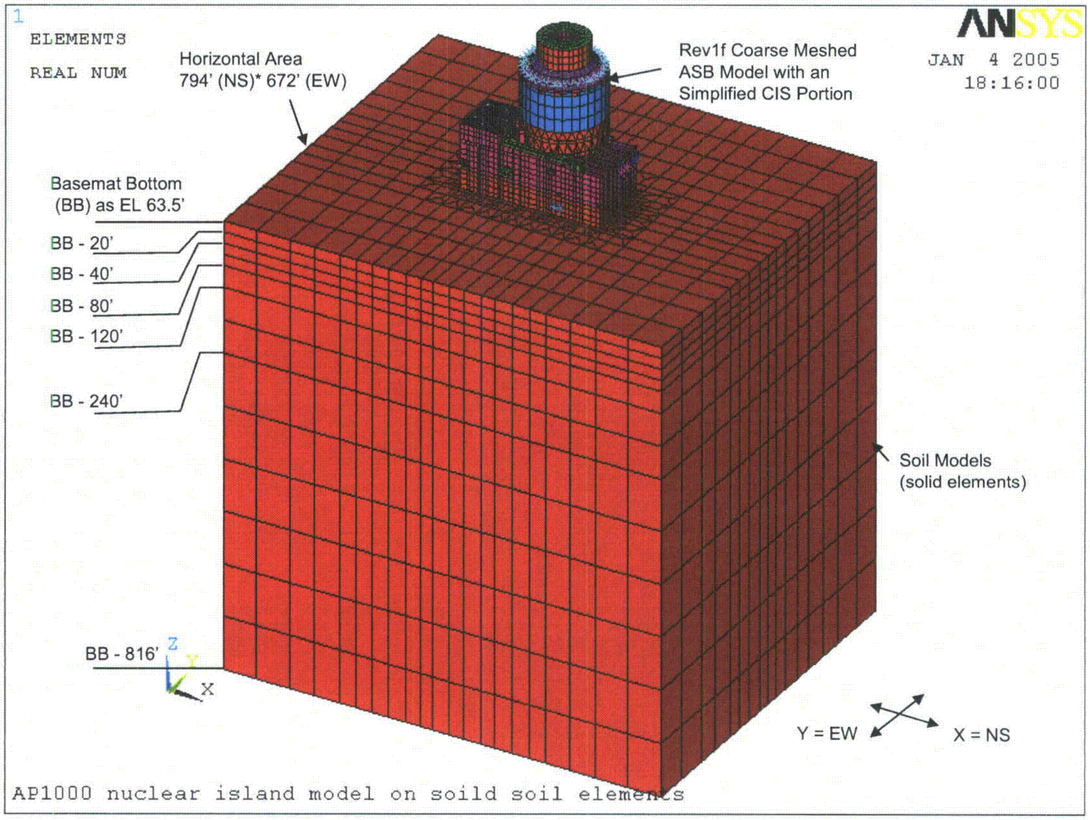

Figure 2.7-1 Analysis Model with Finite Element Models of Soil (No Embedment Case)

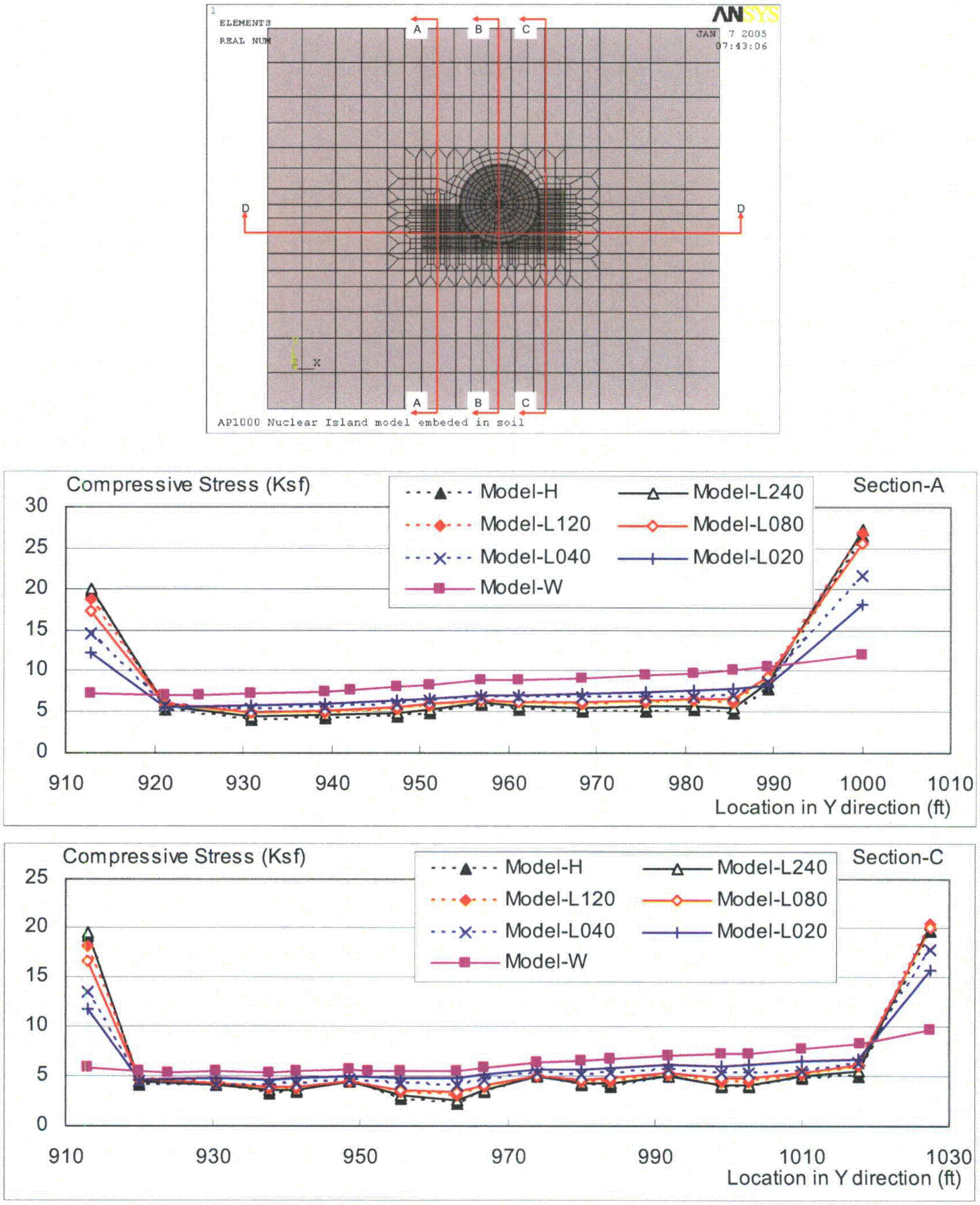

Figure 2.7-2 Comparison of Vertical Stress at Basemat Bottom Node – No embedment

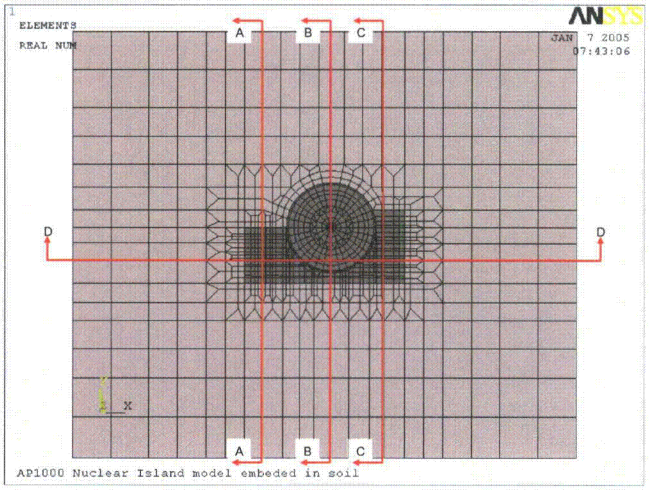

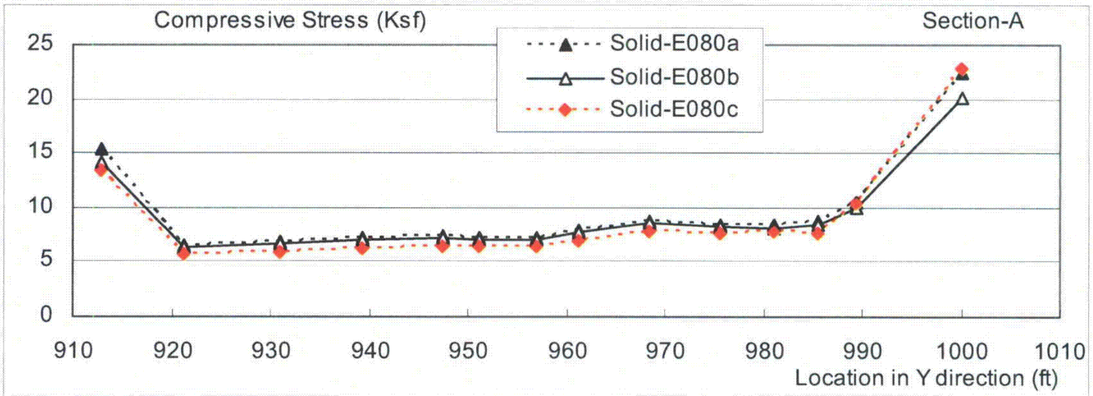

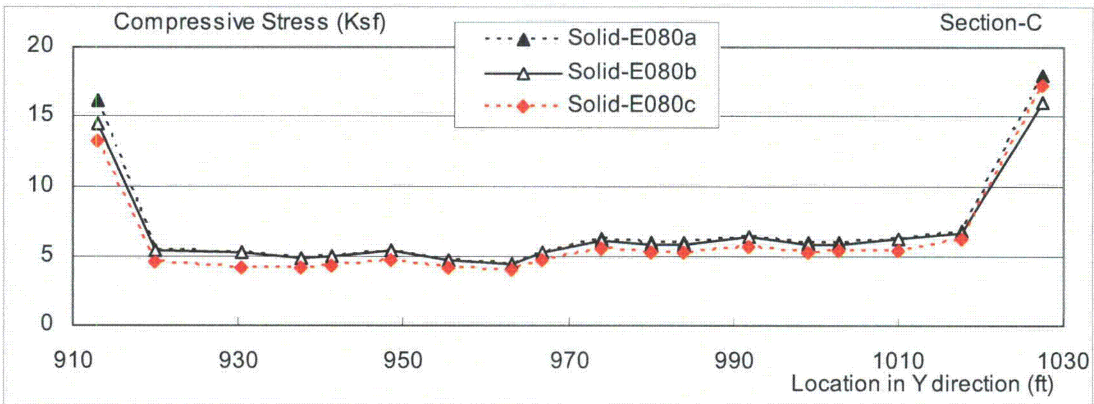

Figure 2.7-3 Comparison of Vertical Stress at Basemat Bottom Node

(Soft to medium soil including embedment)

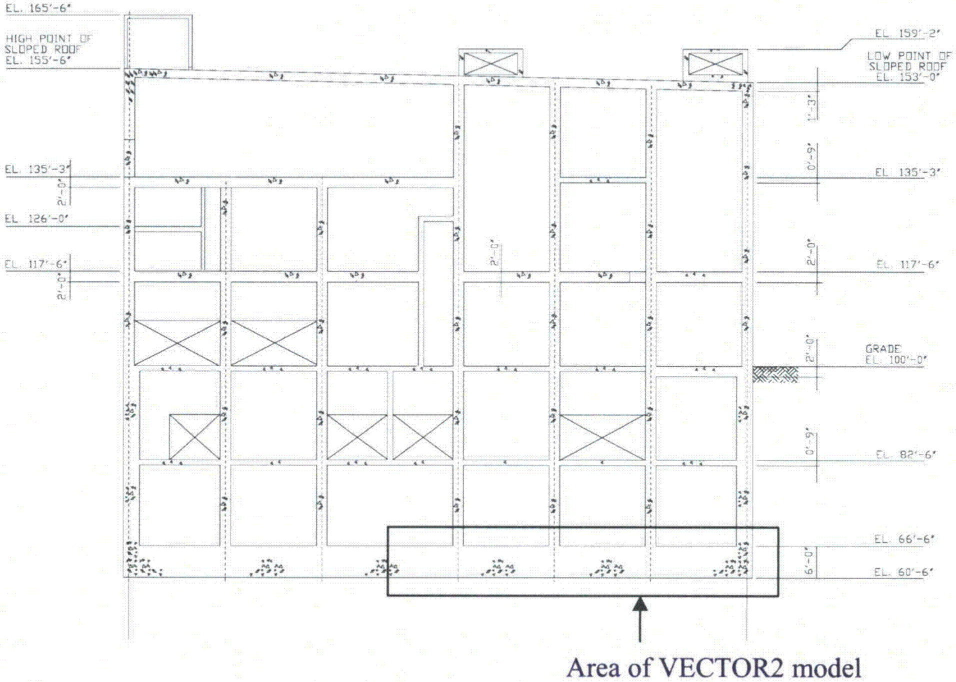

Figure 2.7-4 Cross section through north end of auxiliary building looking south

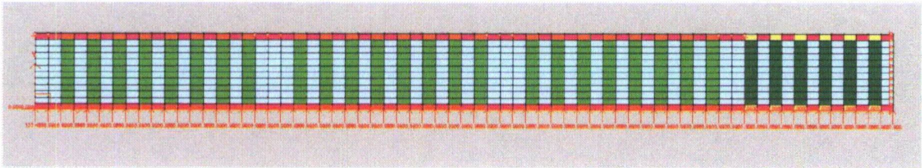

Figure 2.7-5 Vector2 model looking north with Uniform Distributed Load (UDL)

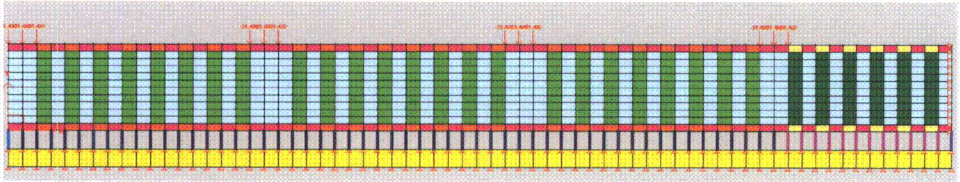

Figure 2.7-6 Vector2 model looking north with Soil Springs

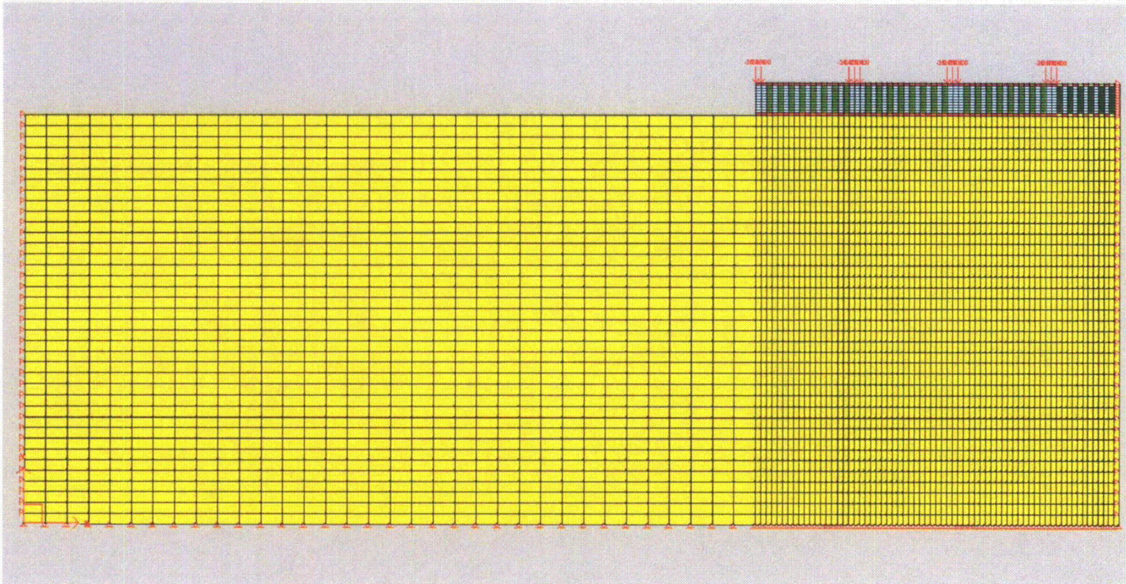

Figure 2.7-7 Vector2 model looking north with Soil Elements

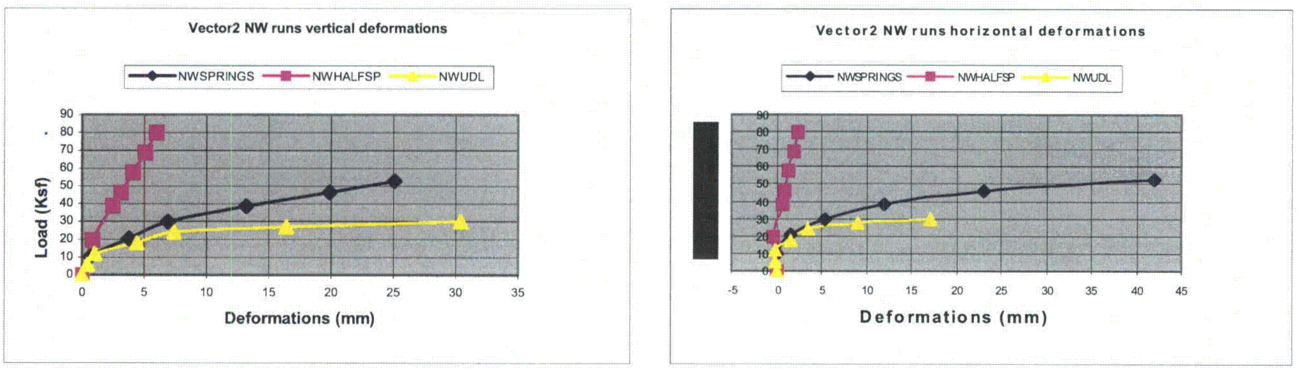

(a) Vertical deformations

(b) Horizontal (dilation) deformations

Figure 2.7-8 Maximum basemat deformations versus average contact pressure

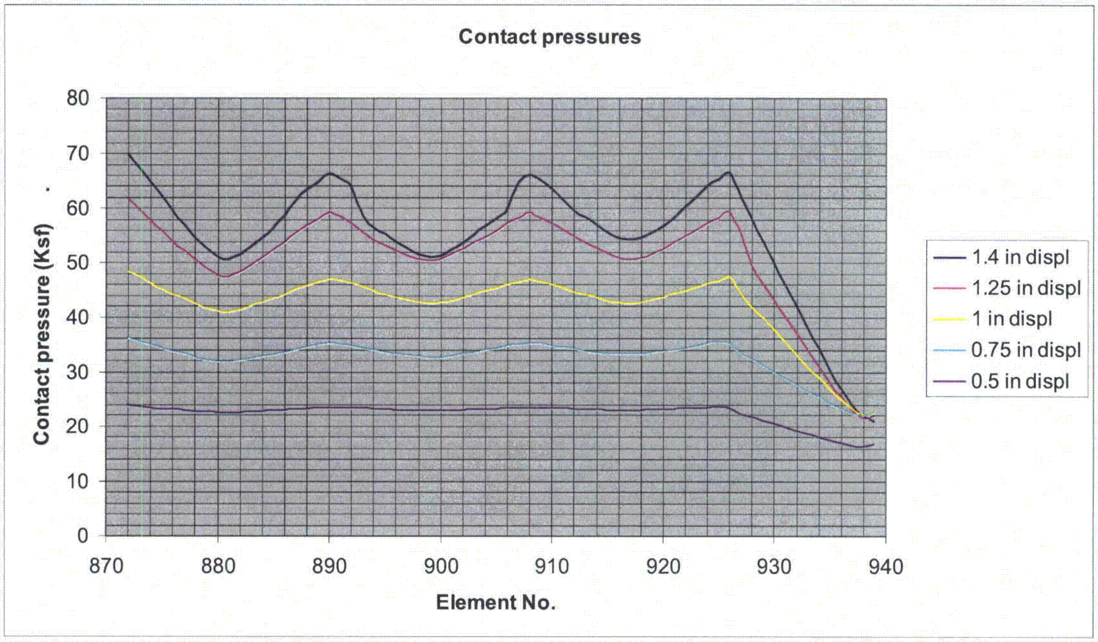

Figure 2.7-9 Contact stresses along mat with Winkler Springs

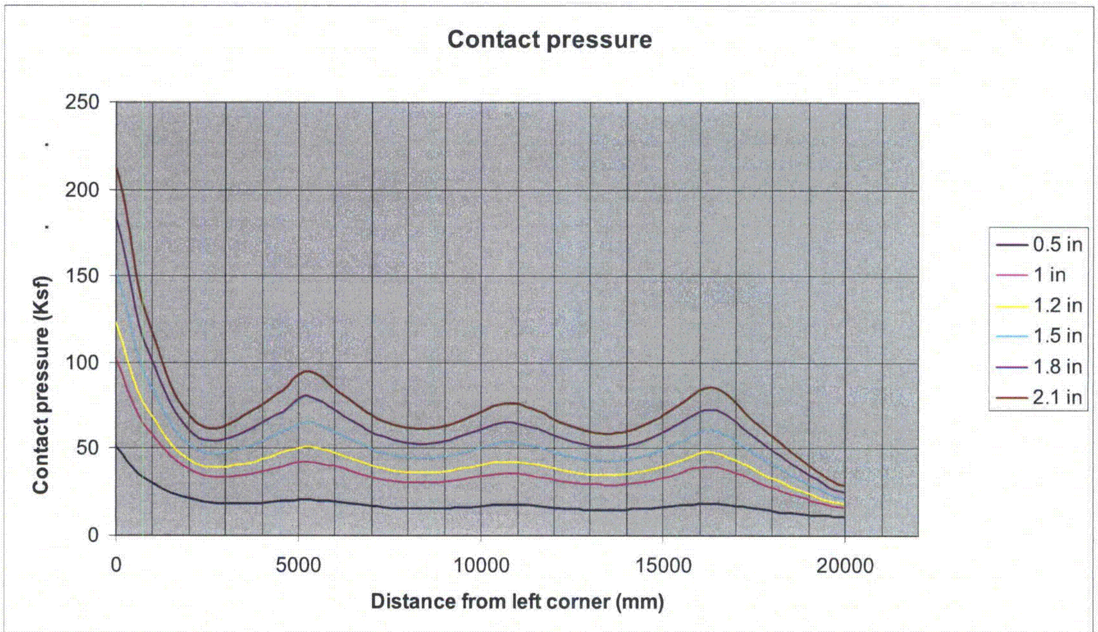

Figure 2.7-10 Contact stresses along mat for Half Space

2.8 Summary of basemat design

The nuclear island basemat has been designed to satisfy the ACI 349 code for the member forces given by conservative analyses. These analyses apply equivalent static loads to a detailed model of the nuclear island on Winkler soil springs. As described in section 2.6.1.2, the loads envelope the seismic response for the worst soil condition. As described in section 2.4.2, the non-linear lift off analyses give very conservative maximum bearing pressures when there is significant lift off. As described in section 2.6.1.1, the soil springs have a stiffness of 520 kcf corresponding to a soft soil site. This spring stiffness is significantly lower than that corresponding to the soft to medium soil case giving the maximum seismic response. Use of the lower stiffness springs is conservative since it maximizes the bending moments in the basemat. The restraint of the side soils is conservatively neglected. Lift off is considered using compression only springs.

The reinforcement in the 6' basemat is sized to have a minimum margin of 20% above that required in the equivalent static analyses on uniform soil springs. This margin was established by studies of the AP600 basemat which has the same configuration as the AP1000. It provides margin to cover variability in the soil properties across the plan of the footprint of the nuclear island.

Studies described in section 2.7.1 demonstrate that the analyses using Winkler soil springs give conservative member forces for design of the basemat reinforcement. Analyses using finite element models of the soil generally showed lower design member forces in the basemat.

Behavior of the basemat for loads beyond the design basis was investigated as described in section 2.7.2. These analyses of the interaction between the basemat and the soil showed ductile behavior of the basemat. As the concrete cracked and subsequently the reinforcement yielded, the deflections of the mat were sufficient to permit significant redistribution of the soil reactions to locations below the walls thus reducing bending moments in the slabs. The final failure mechanism was a shear failure close to the walls at a loading of about three times the SSE design load.

2.9 Nuclear island stability

The 2D SASSI reactions (NS and EW shear, and vertical) are used to obtain seismic response factors between the hard rock case to the upper-bound-soft-to-medium (UBSM) soil case, and the soft-to-medium (SM) soil case. These factors are used to adjust the hard rock (fixed base) NI20 ANSYS seismic time history analysis base reactions to reflect the seismic response for the other two potential governing soil cases UBSM and SM. The shear and vertical loads obtained from the 2D SASSI analyses given in Table 2.4-2 are used to adjust the hard rock (HR) reaction forces and moments obtained from the time history ANSYS analysis to reflect the change in seismic response due to the other soil cases. As seen from this table the upper bound soft to medium (UBSM) and soft to medium (SM) soil cases along with the hard rock case are the controlling generic soil cases. Therefore, it is not necessary to consider the other soil cases. The hard rock time history analysis base reactions are adjusted using the NS, EW, and vertical factors shown in Table 2.9-2.

Passive soil resistance is not considered for overturning seismic stability evaluation. For sliding, the amount of passive soil resistance, if required, is calculated to obtain the minimum factor of safety of 1.1. The deflection necessary to obtain the required passive pressure is then determined to show that it is reasonable (e.g., less than 2").

The factors of safety associated with stability of the nuclear island (NI) are shown in Table 2.9-1 for the following cases:

- Flotation Evaluation for ground water effect and maximum flood effect
- The Nuclear Island to resist overturning during a Safe Shutdown Earthquake (SSE)
- The Nuclear Island to resist sliding during the SSE
- The Nuclear Island to resist overturning during a tornado/wind/hurricane condition
- The Nuclear Island to resist sliding during a tornado/wind/hurricane condition.

The minimum stability factors of safety values are reported in Table 2.9-1. The method of analysis is as described in subsection 3.8.5.5 of the DCD and the coefficient of friction of 0.55 is used. The friction value in the soil below the mudmat has an angle of internal friction of 35°. The Combined License applicant will provide the site specific angle of internal friction for the soil below the foundation.

The factors of safety for sliding and overturning for the SSE are calculated for each soil case for the base reactions in terms of shear and bending moments about column lines 1, 11, I and the west side of the shield building at each time step of the seismic time history. The 2D SASSI reactions (Fx, Fy, and Fz) are used to obtain seismic response factors between the hard rock case to the upper-bound-soft-to-medium (UBSM) soil case, and the soft-to-medium (SM) soil case. These factors were used to adjust the hard rock time history to reflect the seismic response for the other two potential governing soil cases UBSM and SM. The firm rock, soft rock, and soft soil cases have higher factors of safety against sliding and therefore not considered.

The seismic time history analysis used the ANSYS computer code and the NI20 model. The minimum stability factors of safety values are reported in Table 2.9-1. For seismic overturning no passive pressure was considered. For sliding partial passive pressure is considered. Two soil cases are considered for sliding, the soil parameters used for design (friction angle of 35°, and submerged weight of 87.6 pcf), and a lower bound soil density (friction angle of 35°, and submerged weight of 60 pcf). For the design case the amount of passive pressure required to meet the 1.1 factor of safety is 40% for the North-South seismic event, and 47% of the East-West excitation of full passive pressure. For the lower bound case the amount of passive pressure required to meet the 1.1 factor of safety is less than 53% for the North-South seismic event, and 64% of the East-West excitation of full passive pressure. The relationship between passive pressure and displacement at grade is obtained based on the methodology given in Reference 10. The relationship between passive pressure and displacement at grade is shown in Figures 2.9-1 and 2.9-2. The maximum Nuclear Island displacement of the Nuclear Island at grade to develop the required passive resistance is 0.5" for the design case, and 2.3" for the lower bound case. These deflections are based on conservative equivalent static analysis. This will result in large deflections since the seismic loads are considered to be constant and do not reflect the short time duration that they exist during the seismic event. A more realistic non-linear analysis with sliding friction elements using a 2D ANSYS model was performed. The 2D ANSYS model that was used to study the basemat uplift (see Subsection 2.4.2). This 2D non-linear model is for the East-West direction. There is no need to consider the North-South direction since the NI deflections calculated to maintain a factor of safety of 1.1 is largest in the East West direction. This model was modified introducing friction elements along the bottom of the basemat and soil media interface. Direct time integration analysis was performed with vertical uplift and sliding allowed. The three cases that have the lowest factor of safety related to sliding were evaluated. These three cases are HR, UBSM, and SM. The seismic input was increased by 10% to maintain the factor of safety against sliding of 1.1. No passive soil resistance is considered. The resulting maximum displacement at the base of the NI basemat (EL 60.5') using a coefficient of friction of 0.55 is 0.12" without buoyant force consideration, and 0.19" with buoyant force considered. This is negligible sliding during the seismic event, and no passive soil resistance is necessary from the backfill (side soil). Therefore, it can be concluded that the Nuclear Island is stable against sliding.

Table 2.9-1 – Factors of Safety Related to Stability of AP1000 NI

Load Combination	Sliding		Overturning		Flotation	
	Factor of Safety	Limit	Factor of Safety	Limit	Factor of Safety	Limit
D + H + B + W	Design Wind					
North-South	14.0	1.5	51.5	1.5	–	–
East –West	10.1	1.5	27.9	1.5	–	–
D + H + B + W_t	Tornado Condition					
North-South	7.7	1.1	17.7	1.1	–	–
East –West	5.9	1.1	9.6	1.1	–	–
D + H + B + W_h	Hurricane Condition					
North-South	10.3	1.1	31.0	1.1	–	–
East –West	8.1	1.1	16.7	1.1	–	–
D + H + B + E_S	SSE Event					
North-South	1.1(2)	1.1	–	–	–	–
East-West	1.1(2)	1.1	–	–	–	–
Line 1	–	–	1.77(1)	1.1	–	–
Line 11	–	–	1.93(1)	1.1	–	–
Line I	–	–	1.17(1)	1.1	–	–
West Side Shield Bldg	–	–	1.44(1)	1.1	–	–
	Flotation					
D + F	–	–	–	–	3.51	1.1
D + B	–	–	–	–	3.70	1.5

Notes:

(1) No passive pressure is considered.
(2) No passive pressure is considered. From non-linear sliding analysis using friction elements the horizontal movement is negligible (0.12" without buoyant force consideration, and 0.19" with buoyant force considered).

Table 2.9-2 – Factors to Apply to Hard Rock Analysis Base Reactions

Seismic Excitation	Upper Bound Soft to Medium	Soft to Medium
NS	0.98	0.92
EW	1.14	1.11
Vertical	1.06	1.14

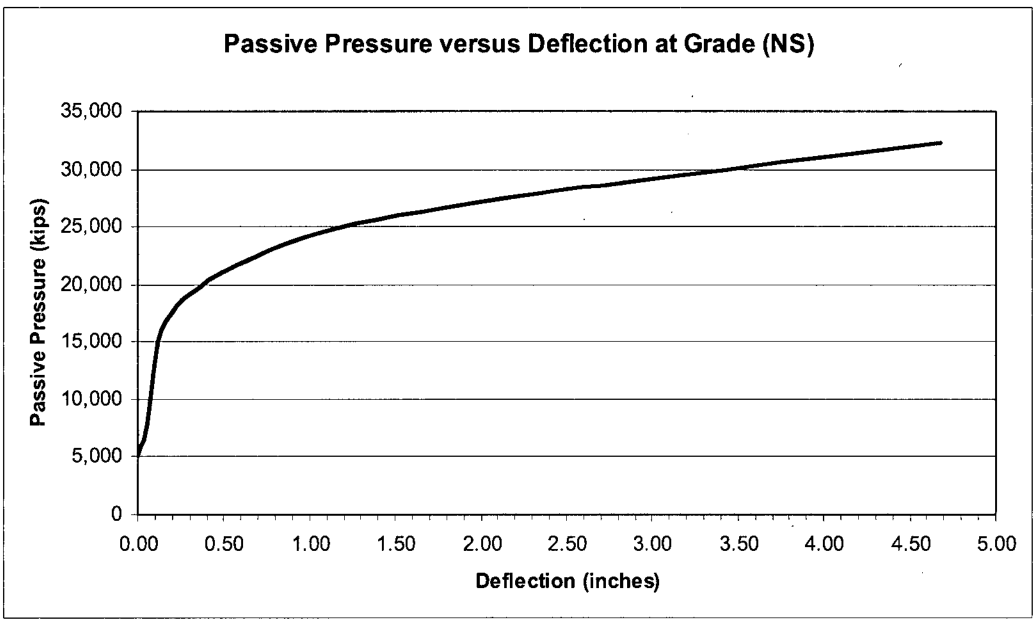

Figure 2.9-1 – Passive Pressure versus Deflection at Grade (North-South Excitation)

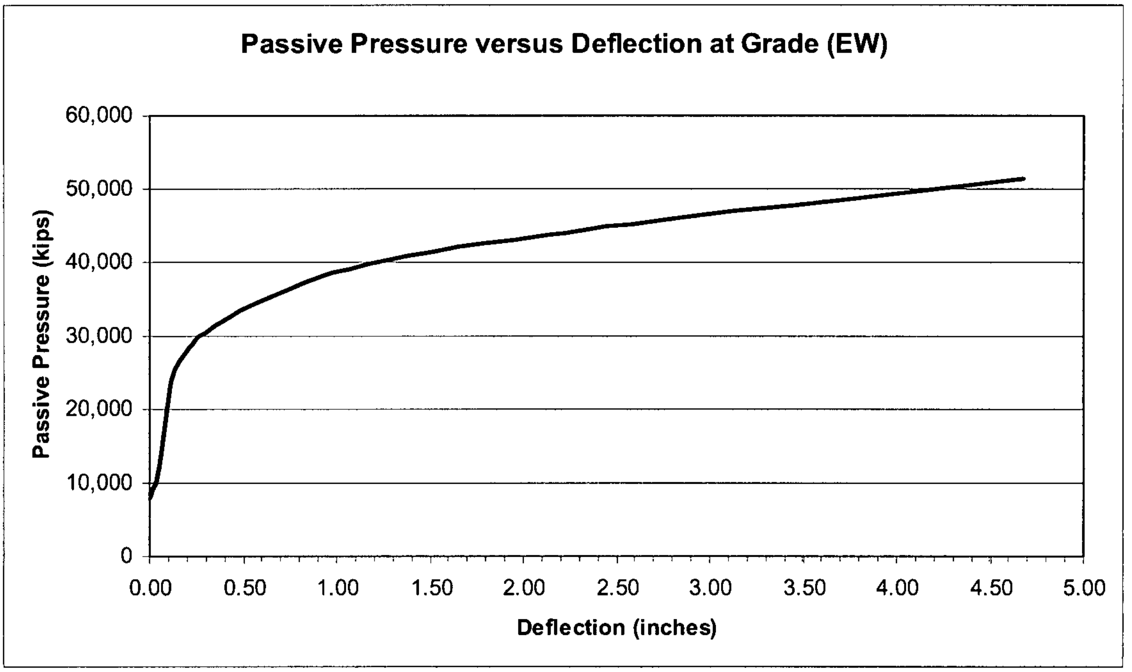

Figure 2.9-2 – Passive Pressure versus Deflection at Grade (East-West Excitation)

3. REGULATORY IMPACT

The design of the nuclear island basemat and evaluation of stability is addressed in subsection 3.8.5 of the NRC Final Safety Analysis Report (FSER, Reference 2) write-ups.

The changes to the DCD presented in this report do not represent an adverse change to the design functions, including the pressure boundary integrity functions and the access function, or to how design functions are performed or controlled. The analysis and design of the nuclear island basemat for soil sites is consistent with the description of the AP600 analysis in 3.8.5 of the AP600 DCD. The changes to the DCD do not involve revising or replacing a DCD-described evaluation methodology. The changes to the DCD do not involve a test or experiment not described in the DCD. The design changes, including the Tier 1 DCD change, will not result in a significant decrease in the level of safety otherwise provided by the design. The Tier 2 DCD changes identified in this report do not require a license amendment per the criteria of VIII. B. 5.b. of Appendix D to 10 CFR Part 52.

The regulations included in 52 Appendix D VIII. A. identify that requests for exemptions from Tier 1 Information by the COL applicants are governed by the requirements in 10 CFR 52.63(b)(1). In addition to requiring that the design change will not result in a significant decrease in the level of safety otherwise provided by the design, the exemption must comply with the requirements of 10 CFR 50.12(a). The criteria of 10 CFR 50.12(a) require that special circumstances are present to grant an exemption. The second of these special circumstances is as follows: "(ii) Application of the regulation in the particular circumstances would not serve the underlying purpose of the rule or is not necessary to achieve the underlying purpose of the rule." Since the underlying purpose of 10 CFR Part 52 Appendix D is to provide for the licensing and construction of standard AP1000 nuclear power plants, an exemption to Tier 1 of the AP1000 DCD to permit application of the Standard AP1000 to a wider range of soils conditions is clearly needed to achieve applicability of the AP1000 to site currently being considered by COL applicants.

The DCD changes do not affect resolution of a severe accident issue and does not require a license amendment based on the criteria of VIII. B. 5.c of Appendix D to 10 CFR Part 52.

The DCD changes will not alter barriers or alarms that control access to protected areas of the plant. The DCD change will not alter requirements for security personnel. Therefore, the DCD change does not have an adverse impact on the security assessment of the AP1000.

4. REFERENCES

1. Not Used
2. Final Safety Evaluation Report Related to Certification of the AP1000 Standard Design, September 2004.
3. APP-GW-S2R-010, Revision 5, Extension of Nuclear Island Seismic Analyses to Soil Sites, February, 2011.
4. Not Used
5. ASCE Standard 4-98, "Seismic Analysis of Safety-Related Nuclear Structures and Commentary," American Society of Civil Engineers, 1998.
6. Not Used
7. ASCE Standard ASCE/SEI 43-05, "Seismic Design Criteria for Structures, Systems, and Components in Nuclear Facilities", American Society of Civil Engineers, 2005.
8. Vecchio, F.J., and Collins, M.P., "The Modified Compression Field Theory for Reinforced Concrete Elements Subjected to Shear", ACI Journal, V. 83, No. 2, 1986, pp 219-231.
9. Vecchio F.J.," Disturbed Stress Field Model for Reinforced Concrete: Formulation", ASCE Journal of Civil Engineering, Vol. 126, No. 9, pp. 1070-1077.
10. HSAI-Yang Fang, "Foundation Engineering Handbook," Second Edition, 1991, Van Nostrand Reinhold